SIMULATION OF RADIATION SOURCE LOCALIZATION THROUGH CIRCLE APPROACH AND 3-D VISUALIZATION OF UNKNOWN ENVIRONMENT USING UGV EQUIPPED WITH 3-D LIDAR BASED ON ROTATIONAL 2-D LIDAR

A Thesis

by

HALIT MURAT DURUKAN

Submitted to the Graduate and Professional School of
Texas A&M University
in partial fulfillment of the requirements for the degree of

MASTER OF SCIENCE

Chair of Committee,	Stavros Kalafatis
Committee Members,	Yassin A. Hassan
	Kevin Nowka
Head of Department,	Miroslav Begovic

August 2021

Major Subject: Computer Engineering

ABSTRACT

Localization, identification, and quantification of radioactive sources in an unknown environment with conventional methods based on a technician carrying a handheld radiation detector, such as the Geiger Muller detector, is considered a time-consuming and hazardous method. Although autonomy is still a question mark for a fast emergency response to accident scenarios such as Fukushima Daiichi, developments in autonomous robotics can be faultlessly integrated into radioactive source searching problems with maximum accuracy and minimum span to protect human workers due to the extremely harmful nature of radiation. A radiation source model of Cs-137 and Am-241 employing Ray-Tracing algorithms as well as Timepix hybrid pixel detector that is exceedingly small, powerful, and capable of measuring has been recently contributed to literature for the first time so that researchers are able to simulate these models and test methods under different conditions even if there is no real detector and source. In this research, the visualization of an unknown environment using a 3D LIDAR based on a 2D rotational LIDAR instead of an available 3D LIDAR, which is still an expensive technology for robotic platforms, has been developed. The circular approach based on a probability density function (PDF) of normal distribution has been presented to estimate the localization of radiation sources in an unknown environment. The Gazebo simulator has been employed to spawn an empty environment and test the circular algorithm using a Timepix detector and Am-241 radiation source. The accuracy and duration results captured from the experiment are compared to similarly available methods in the literature. The circular method is competitive in terms of duration to estimate the source position.

Unmanned Ground Vehicles (UGVs) have an extremely high level of accuracy advantage in estimating a point source's actual position. This advantage is preserved in the circular approach.

DEDICATION

For my parents who raised me at the expense of countless self-sacrifices and my government which gave me this opportunity…

ACKNOWLEDGEMENTS

I would like to express my sincere appreciation to my advisor, Prof. Stavros Kalafatis for his support, guidance, valuable comments, and suggestions throughout this study. Additionally, I would like to thank the committee members for their guidance and feedback. This thesis has been supported by Ministry of National Education and this research is co-advised by the Turkish Atomic Energy Authority. I would like to express my deepest gratitude to my deepest one for her endless support, patience, and love. Finally, I am thankful to my family for their trust, encouragement, and patience. None of this would have been even possible without their support and love.

CONTRIBUTORS AND FUNDING SOURCES

Contributors

This work was supported by a thesis committee consisting of Professor Stavros Kalafatis and Professor Kevin Nowka of the Department of Electrical and Computer Engineering and Professor Yassin A. Hassan of the Department of Nuclear Engineering. All other work conducted for the thesis was completed by the student independently.

Funding Sources

Graduate study was supported by a scholarship from the Ministry of National Education in Turkey.

TABLE OF CONTENTS

Page

LIST OF FIGURES

Page

1. INTRODUCTION

Developments in robotics gain importance in filling gaps in engineering and impacting almost all disciplines from agriculture to nuclear engineering. Although incredible advancements in robotic science have been introduced, each robot platform needs to be designed according to the application. Special design requirements are the most problematic disadvantage of robotics because the increased level of diverse applications requires a plethora of multi-disciplinary approaches to solve problems. Another reason why advancements in robotics are important is because robots can reduce physical exposure of humans to potentially dangerous situations such as nuclear accidents that can generate high levels of radiation i.e. nuclear accidents generating high levels of radiation. The stochastic nature of radiation sources harms the human body due to particles and rays, including a high energy level like gamma rays. For example, the well-known nuclear accident Fukushima Daiichi that occurred in 2011 caused an evacuation of about 150,000 people from the Mayak site as a result of radioactive contamination from the damaged reactors. Radioactive isotopes released into the Pacific Ocean contaminated tons of water during and after the accident. It is the most severe nuclear accident in literature since the Chernobyl disaster in 1986. After these accidents, the nuclear industry leveraged the help of the robots to measure, localize, identify and quantify radiation sources, collect samples from razed buildings, and estimate the reasons behind the accident. Due to the high level of radiation and absence of shielding, numerous attempts failed. Experts believed that autonomous robots might be beneficial, however, this demand caused the usage of more electronics, so the failure rate increased. Nevertheless,

autonomy is one of the most popular researching areas in robotics in order to make the robots more capable of achieving missions without a labor force. However, autonomy causes new limitations in investigations of nuclear accidents because the concrete used in the construction of nuclear facilities is very thick and obstructing to GPS and Wi-Fi usage. Autonomous platforms also come with battery life limitations and the problem of identifying an environment, which is an area still being researched in the robotic community. The uncertainty of the environment in such a scenario makes the identification harder. Another main disadvantage of autonomous robots is that more electronic requirements sensitize the platform to the high level of radiation, so more shielding is required to be robust enough against radiation sources. The stated reasons support the logic of usage of tethered communication coming with distance restriction. Tethered communication also has an advantage in terms of fast radiation detection with the help of the operator's experience. Nevertheless, during or after disasters, high radiation isotopes make this type of investigation almost impossible. Type of desired application can balance the trade-off between autonomous robots and tethered robots. Fortunately, autonomous robots can be reasonably employed in the presence of a relatively lower level of radiation that is harmful to humans, for instance, homeland security and radioactive mining searching. The current methods of localization of radiation sources in an environment depends on the physical labor force. A technician or worker does the radiation measurement with a handheld detector such as Geiger Muller (GM) detector. According to U.S.NRC, the annual total effective dose rate is five rems, which one rem is the average dose received in three years of exposure to natural radiation. In order to decrease the

radiation dose to the human body, a technician or worker can be replaced by autonomous robots with a radiation detector in nuclear facilities. A combination of a worker and a semi-autonomous robot might be an alternative solution if the environment and radiation level are known. In case the communication between operator and the robot is suddenly cut off, the autonomy takes initiative. Most cases do not meet these conditions; however, the region of interest (ROI) needs to be regularly inspected. An expert should frequently investigate these inspection results to protect the humans around the nuclear site and envision possible radiation leakage in a compartment such as pipes in a reactor. Thus, the experts could take precautions in advance. Robots with a camera or LIDAR also offer a solution to the following problem: the map of construction is outdated or subject to change in time. Currently, localization and mapping (SLAM) algorithms can visualize the unknown environment during in-situ measurement. SLAM algorithms are a very well-known research topic in robotics research. There are numerous SLAM algorithms employing different sensors which have both advantages and disadvantages. The algorithms with LIDAR provide more accuracy while the algorithms with a camera ensure a color map of the environment. 3D LIDAR in particular is still an expensive technology and needs higher budgets to be developed for robotic applications. Another main problem of the 3D LIDAR is that it needs a more powerful computer, which increases the research budget. To reduce the computational cost that weakens the battery performance during the mission, less complex hardware should be chosen. Battery management is crucial in the localization and identification of radiation sources in an unknown environment through an autonomous robot because of the numerous electronics employed by

the designer. As well as the SLAM algorithms, path planners are responsible for the movement of the robot platform concerning the desired path in the map. The collected data during the mission can direct the agent or the agent can be directed by a predefined roadmap in the known map. In the former, a robot with the radiation detector can detect and avoid the obstacles so that it follows an updated course line in order to converge the radiation sources with the help of count readings from the detector. In latter, once the map of the unknown environment through SLAM techniques is obtained, mobile robots through waypoints can be directed. Both methods have some positive and negative aspects, but the detection efficiency needs to be taken into account. The collected data method may be better for fast-emergency responses while it does not inform the experts about the general radiation distribution in the environment. The predefined map approach can be considered a time-consuming event. However, it might be developed by the choice and implementation of the correct algorithm as the general exploration of the environment is preserved. Awareness of the obstacles in the environment is also maximized. Dimensional developments in radiation detectors allow researchers to solve the integration problem of detectors to the robotic platforms to be employed in situ measurements. For example, the payload capacity of Unmanned Aerial Vehicles (UAV) is still unknown for flight longevity, so new type small detectors such as Timepix can be considered as a beneficial tool. In parallel to the developments in the detectors, the shielding techniques progress, which are helpful for human workers to be replaced by the robotic platforms.

1.1. Literature Review

In 2008, a researcher developed two different motion planning strategies called gradient-based Bayesian method and a sequential-based Bayesian method to build a radiation map. The first method offered a solution based on uncertainty metrics without a predefined path so that the robot could potentially visit the region of interest (ROI). In contrast, the second method allowed the robot to visit all cells in the predefined map once and provided optimal time [1]. In parallel, detection and estimation of multiple radiation sources using counts from multiple sensors were handled using Bayes factors and a Monte Carlo technique [2]. Similarly, Baidoo-Williams had introduced some theoretical approaches to be adapted to unmanned platforms [3]. The researcher focused on the perfection of the sensor readings not being possible in reality and combined it with the maximum likelihood approach. The multi-resolution method improved Baidoo-Williams's results [3]. However, the results still depended on the perfect count reading of multiple detectors [4]. The localization problem was handled by employing different approaches like the spatial statistical method [5]. In this method, detectors counting particles from radiation sources with the Poisson distribution model and maximum likelihood estimates of the strength and location of the source were used. Robots had adapted radiation detection systems thanks to the incredible increase in the commercialization of robotic platforms. One good example for this adaptation to contour the radiation map in 3D space was introduced by Han [6]. Another study for a relatively low radiation source presented a methodology with inexpensive, small UGV employing a scintillation detector with rotational capability [7]. The peaks from directional counts were used to navigate the robot

to the radiation source autonomously. A robotic platform based on a grid-based algorithm searching radiation sources in the environment with predefined waypoints with the Geiger Muller detector was considered. The environment was empty, and the map was needed to be known to the robotic platform [8], but the map of the environments is generally out of date, which made the study less realistic. In many works, it had been assumed that the environment was empty so that an attenuation-free environment was considered. In study of H.Lin and H. J. Tzeng , an artificial potential field was integrated into a mobile robot [9]. A particle filter employed attractive forces with the help of a sensing model, which showed that the robot could converge to the position of the source with less error. As well as this contribution, an environment having two obstacles with the radiation attenuation coefficient instead of space was used. As the sensor technologies have been improved in terms of efficiency of battery usage and resolution and affordability, more applications with new techniques of computer vision in robotics are emerging. Application of the Simultaneous Localization and Mapping (SLAM) algorithm with LIDAR or depth camera can be considered as a good example. One of these studies concentrating on Visual SLAM (VSLAM) showed the capability of serving in a totally unknown and potentially contaminated environment to localize, identify and quantify the radiation source in the 3D radiation map [10]. This novel study comes up with a realistic approach at the expense of a high computational cost and expensive hardware. Advances in data processing allowed SLAM algorithms to be merged into 3-D visualization of radiation. The concept of 3-D Scene-data fusion with 3-D LIDAR and gamma camera made the radiation itself visible [11]. The 3D reconstruction of the

radiation in space using SLAM and MLE through a mobile robot with a Compton camera was visualized [12]. The author introduced the SLAM and determined an algorithm based on the detector's multiple viewpoints and pose. For high radiation scenarios like the Fukushima Daiichi accident, fast emergency robots were required, but none of them using wireless communication achieved the mission due to more shielding requirements. An exhaustive summary of the mobile rescue robots and a review of ground-based robotic systems took part in the literature, respectively [13][14]. Also, D. K. Wehe highlighted a summary of the importance of robotics in the nuclear industry [15]. This novel summary allowed researchers to have enough background and figure out the challenges of usage of robots in the radiation industry. One of the difficulties after a nuclear disaster is collecting samples from the debris to explore and figure out the reasons behind the disaster. The inspection of the radiation level of the environment should be regularly performed to reduce the risk of possible leakages, for example, in the pipes of a nuclear facility. A humanoid robot with a radiation detector controlled by a joystick controller was modeled to emphasize the importance of inspection and sample collection [16]. Furthermore, a decommission plan for the Fukushima reactor was simulated in order to be able to allow the researchers to estimate the position and the amount of radiation through the gamma-ray CT method [17]. The source positions were theoretically estimated. Another main problem in the presence of a high level of radiation is how the region of interest (ROI) affected by the radiation is contoured. In such an environment, the single source assumption can not be used due to numerous sources. As a reasonable answer for this question, R. Newaz introduced an efficient exploration method using topographic

maps and Bayesian methods through a UAV [18]. In light of this study, two methods, Variational Bayesian and Hough Transform, for optimizing the radiation contour were tested and contributed to the literature of the robotic systems for radioactive mission by the Redwan Newaz in a study of UAV-based multiple source localization and contour mapping of radiation fields [19]. For the localization of radiological sources in a predefined area, autonomous and non-autonomous approaches have been introduced. The study of Vazquez-Cervantes was offering an empirical approach with a human-controlled robot carrying NaI and Hyper Pure Germanium detector [20]. At the same time, T. Lázna came up with autonomy to reduce the interaction between worker and radiation exposure and time required with the help of an algorithm developed [21]. In another study, radiation-searching research utilizing Recursive Bayesian Estimation (RBE) had been introduced. The developed method had the ability to search for multiple radioactive sources and identify the isotope as a result of a couple of measurements in an unknown environment [22]. This research was recently expanded to the presence of attenuation in the radiation model, optimized using Fisher information, and the robot platforms were varied by the same authors [23]. A very similar method employing Bayesian framework using a particle filter and Fisher information was handled by B. Ristic to search for the radiation source in an environment [24]. In parallel to the popularity of the TurtleBot robot platforms being affordable and having an easy framework among the robotic community, the adaptation of nuclear instruments and different algorithms became popular like in the research presented “Autonomous Search of Radioactive Sources through Mobile Robots”, where Markov decision process was implemented to wisely navigate the

robot to the radioactive source [25]. A tracked robot was modified by the radiological instrument unit and the robotic arm to collect a sample from the debris and hardly shielded for dismantling and decommissioning operations. It was developed to be employed in CEA nuclear facilities as an example of a non-autonomously controlled robot [26]. This novel study would be considered as a reference work among the robots using tethered communication needing the experience of an expert to be navigated for the realistic inspection before a disaster; however, the distance limitation is a hint that the applicability of the robot does not allow the worker to be protected in the presence of intense radiation. For the terrestrial radiation mapping, usage of only UAV platforms would decrease the precision of estimation of sources to have a better period for the inspection of all the regions of interest. P. Gabrlik and T. Lazna illustrated that the UAVs are best for exploring the largest area while the accuracy highly depending on the well-known inverse square law is lower [27]. In most cases, only the gamma-ray monitoring was minded while the researcher presented a UAV carrying a gamma and neutron sensor [28]. The platform had an Odroid computer communicating with GPS Receiver and Antenna. Although the UAV is not common for indoor applications, two different methods using voxel mapping in a GPS-denied environment and a waypoint selection algorithm were suggested for a single radioactive scenario [29]. The accuracy was less than 1.52 m, which is acceptable for an indoor application through UAV. Then, the study was expanded to the distribution of multiple sources [30]. The most interesting contribution to the robotic community in terms of radiation sensor and the source was provided in the study of "Localization of Ionizing Radiation Sources by Cooperating Micro Aerial

Vehicles With Pixel Detectors in Real-Time" because a realistic model of Cs-137 and Am-241, and an interface for Timepix detector, for the first time, had been gained to the ROS community in order to be able to test the developed methods even if the researcher does not have a real radiation source and a detector [31]. This novel study gives an incredible tool to beginners with limited background about nuclear areas. The research presented also indicated that micro-UAVs with extremely small and hybrid semiconductor Timepix detectors can be employed to localize and map radiation. Multi-robot disciplines, including a UAV team, a UGV team, or a mixture of UAV and UGV, can act indoors and outdoors. Multi-robot systems needed to be considered to decrease the response time and utilize the advantages of different robots while the accuracy was being preserved. For this reason, the estimation problem in the presence of multiple radioactive sources was considered with the help of a particle filter algorithm and a source separation approach. This study was supported by frontier-based exploration to minimize the exploration time and area pruning algorithm to ignore areas with low radiation intensity levels so that the distance between unexplored region and robot was minimized [32]. A good combination of robots and a human operator was handled to allow the robotic team to have faster response time and more accuracy [33]. In such an approach, each robot is responsible for its own mission. The requirement of a human operator has been kept minimum. The accuracy in this study was improved by the Gauss-Newton optimization later on [34]. All the improvements presented, and aerial photogrammetry tools were gathered in order to minimize the importance of the human operator and interfere in case of radioactive hazard. Similar research as another example of a multi-robot system to

test the Fourier scattering transform and Laplacian eigenmap algorithm over the dataset from the region of Savannah River National Laboratory was presented, and the active exploration algorithm navigated the robotic platform. By commercializing the Compton camera in parallel to the developments in robotics, a robotic project using Compton camera and voxel grid-based mapping approaches together was illustrated [35]. Still, the budget of the project was highly neglected due to the utilization of the Compton camera. On the other hand, the first man-packable Unmanned Surface Vehicle to inspect the cooling ponds and connected streams in a debris-free environment using a spiral path and sampling method was presented in the study of "A man-packable unmanned surface vehicle for radiation localization and forensics" [36].

1.2. Motivation

Conventional methods to search for radiation sources is risky for the health of human operators because the search of the radiation source in an unknown environment is empirically done by a human operator having a handheld radiation detector like a Geiger-Muller. If any radioactive sources have been detected, it can be easily located by the technician, but the invisibility of radiation can do harm to the tissues of the human body. Fortunately, the developments in robotics make the human operators possible to be replaced by the robotic platforms, according to the requirement of the application. The visualization of the environment is another key point to have an idea about the unknown environment to both successfully complete the mission and accurately estimate the position of the source. In the literature, there have been numerous works employing the SLAM algorithm and gathering the radioactive information with SLAM. These novel studies

offer a good visualization of the environment including both radioactive and structural information, however, the computational cost makes it less reliable to monitor the radiation level in situ measurements. To map the environment in 3-D using SLAM methods, a depth camera or 3-D LIDAR is required. Due to the affordability of the camera and still high expense of 3-D LIDAR technology, many works employing a camera are available in the literature. On the other hand, the 2-D SLAM algorithms are also applicable to the real scenarios thanks to the affordable sensor prices of 2-D LIDAR. A recent research providing the Gazebo model of Cs-137 and Am-241 as an open source to the Robot Operating System (ROS) community for the first time so that that researchers are then able to develop and test new searching algorithms in case of even an absence of a real source and detector [31]. Path planners do not perfectly follow the pre-defined path, and the error between actual and pre-defined path is observed, so the orientation of the detector with respect to the radiation source cannot be used as perfectly reliable information. The reasons explained above motivate us to utilize the benefits of sensors and methods individually to design a realistic robot platform to be employed under a realistic situ measurement. In this research, a TurtleBot3 mobile robot with a 3-D LIDAR based on the rotational 2-D LIDAR with a pan-tilt mechanism and Timepix detector in Gazebo Simulator has been employed. During the study, waypoints are used to navigate the robot, and an unknown environment through the point cloud is visualized in 3-D. For the localization of radiation source, the circular algorithm is developed. As a result of this study, we aim to develop an algorithm to search for the radioactive source in an unknown environment, and then combine this algorithm with low-cost hardware having low

computational cost so that the total cost of the robotic platform decreases. In parallel, the less electronics for less shielding are employed.

1.3. Radiation Background

Statistics apply to the measurement of ionization and the understanding of variation that occurs in radiation counting. It also serves as a check on a system because a set of measurements under similar conditions should statistically have the same result. If results differ from predictable statistical fluctuations, one can assume the problem is in the counting system. Counting statistics can be used to estimate the accuracy of a single measurement. Statistical distributions can identify precision. For radiation detection, counts are proportional to decay of source, which means that the higher the activity causes the higher the counts. Radioactive decay is a random event; for example, if two identical counts are taken in sequence on a sample of a long-lived radioisotope, the counts will almost always differ even though the activity of the sample is essentially unchanged. There are three main distributions: Binomial, Poisson, and Gaussian, respectively, to be used in radiation counting. For radioactive material, the atom decays or does not decay (binomial), a large number of atoms in a material decays (Poisson), and the number of counts is greater than 25 (Gaussian). The normal distribution is:

$$P(x) = \frac{1}{\sqrt{2\pi \mathrm{x}}} e^{-\frac{(x-\underline{x})^2}{2\underline{x}})} \quad (1)$$

where $\underline{x}$ is the mean value of the distribution. Two important properties of a normal distribution are that the distribution is symmetric concerning the mean value.
Hence, *P(x)* depends on the absolute value of the deviation of any value x from the

mean, and the distribution is slowly varying [37]. The standard deviation of the normal distribution is:

$$\sigma = \sqrt{x} \tag{2}$$

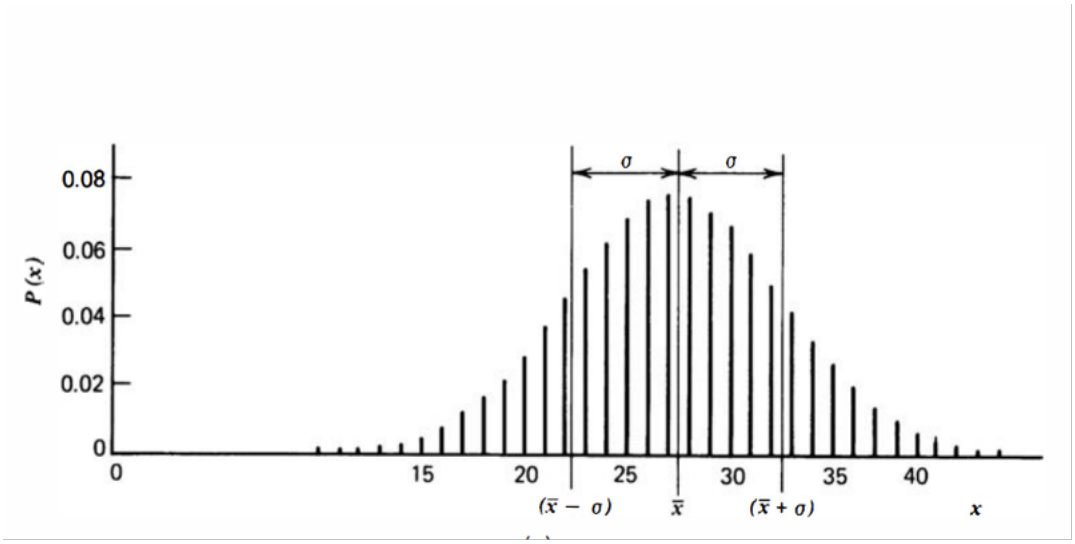

Figure 1. Normal (Gaussian) Distribution [37]

It is known that the detectors are modeled by Poisson distribution. However, the normal distribution Probability Density Function (PDF) can be employed due to high value in Poisson (Figure 1). This value is the mean of count readings in our case, causing a similar behavior with Normal distribution. Error propagation is another important thing in radiation counting because variables with associated errors must account for those errors. Operations (adding etc.) carried out counting data that were originally Gaussian distributed to produce a Gaussian shape. The error propagation formula for all operations is:

$$u = \int (x, y) \tag{3}$$

$$\sigma_u{}^2 = (\frac{du}{dx})^2\sigma_x{}^2 + (\frac{du}{dy})^2\sigma_y{}^2 \quad (4)$$

Where;

u: derived quantity

x,y: directly measured counts

$\sigma_{x,y}$: standard deviations of x,y

For simplicity,

$$\sigma_{x+y} = \sqrt{\sigma_x{}^2 + \sigma_y{}^2} \quad (5)$$

Although there have been numerous interaction mechanisms for gamma-rays, three main types are important (Photoelectric absorption, Compton scattering, and Pair production). Among those, photoelectric absorption is the predominant interaction at energy levels. A photon undergoes an interaction with an observer atom in the photoelectric absorption process, where the photon completely disappears. In its place, an energetic photoelectron is ejected by the atom from one of its bound shells. The interaction is with the atom as a whole and cannot take place with free electrons for gamma rays of sufficient energy. The most probable origin of the photoelectron is the most tightly bound or K shell of the atom. The interaction process of Compton scattering occurs between the incident gamma-ray photon and an electron in the absorbing material. In Compton scattering, the incoming gamma-ray photon is deflected through an angle concerning its original direction. The photon transfers a portion of its energy to the electron, which is then known as a recoil electron. If the gamma-ray energy exceeds twice the rest-mass energy of an electron (1.02 MeV), the process of pair production is

energetically possible. At gamma-energies that are only a few hundred keV above this threshold, the probability for pair production is small [37].

Radioactive material emissions are categorized into six subbranches: gamma radiation, X-rays, beta β particle, alpha α particle, neutrons and emits infra-red (heat) radiation. Gamma radiation comes from the nucleus and is known as highly penetrating. It is also monoenergetic, and energy above a few keV is easy to discern. Gamma radiation travels meters in the air, and high z material is needed for shielding. X-rays are monoenergetic and similar to gamma rays. Beta particles come from the nucleus, and the range is feet in the air while it is not monoenergetic distinctly. Alpha particles ionize greatly and are monoenergetic. The energy of alpha particles is discernible with special spectrometry. Alpha particles can travel just a few cm in the air due to their heavy structure and can be shielded by the dead layer of skin. Neutrons are the most problematic among the emissions because of spontaneous fission. Neutrons' range in air is very long. Low z materials are used in moderation, and the energy of neutrons is not discernable. Since the primary source of infrared radiation is heat or thermal radiation, any object having a temperature radiates in the infrared. Even objects that we think of as being very cold, such as an ice cube, emit infrared. Nuclides can emit combinations of all radiation.

Numerous types of detectors are available in the industry. The main types of detectors can be divided into three main branches: gas-filled detectors, semiconductor detectors, and scintillation detectors. Gas-filled sensors operate by utilizing the ionization produced by radiation as it passes through a gas. It consists of two electrodes to which a particular electrical potential is applied. Space between the electrodes is filled with a gas,

and ionizing radiation loses energy to the gas by creating excited molecules and generating electron-ion pairs that have positive ions and electrons. On average, about 30-35 eV of energy is lost per electron-ion pair made. These charges would recombine without an external electrical field. The detector signal is generated by the motion of charge in the electric field. Scintillation and semiconductor detectors can provide gross count and spectral information. The gross count can find the localization of radioactive material as spectral data is used to identify. In parallel, spectral information and gross count together are beneficial for the quantification of the material.

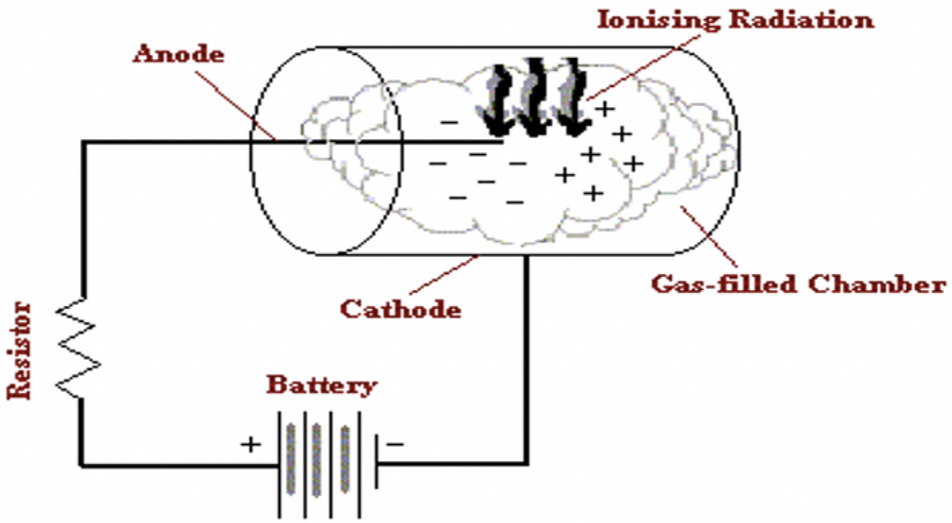

Figure 2. Structure of gas-filled detector[37]

In semiconductor detectors, electrons and holes are created, and these pairs have been pulled apart by the electric field. The charges collected derive a change in voltage, and these changes are turned into the signal (Figure 2). Hybrid semiconductor detectors like Timepix are used to detect ionizing detectors, which may visualize tracks of particles interacting in the semiconductor pixelated sensor bump bonded to the Timepix

readout chip. Energy deposited in the individual pixels and properties of these tracks enable us to classify the incident radiation and to assign the correct conversion coefficient between several detected events and the desired quantity (Figure 3).

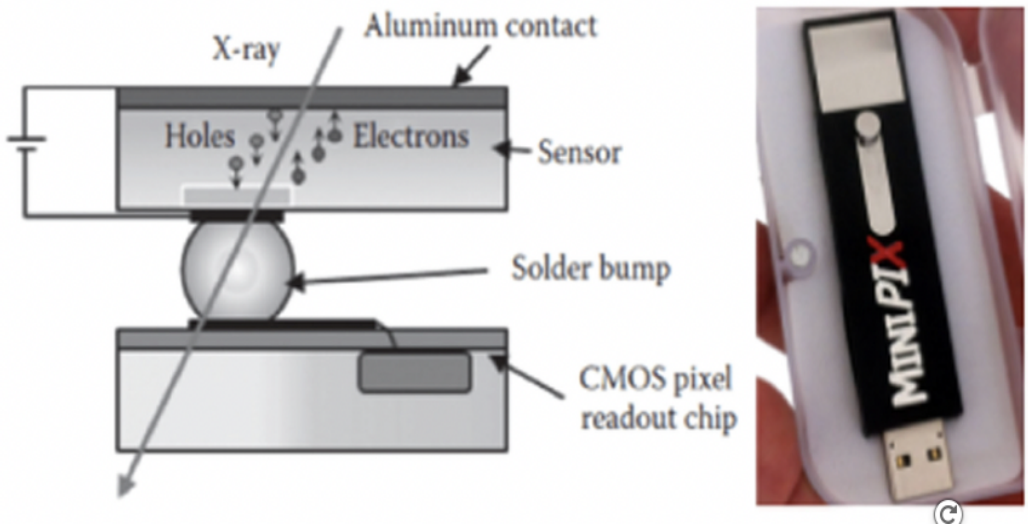

Figure 3. Innel pixel structure (left) and MiniPix (right) [31]

In scintillation detectors, gamma rays trigger the electron. Then, the electron passes the photocathode and hits the dynodes in PMT. Visible light is observed in PMT during this process. Scintillators convert the energy of charged particles into detectable light with high scintillation efficiency. Conversion should be linear, which means that light yield is proportional to deposited energy. The medium should be transparent to light, and the decay time of luminescence should be short for fast signal pulses. It should construct a detector of generous size and index of refraction near the glass to permit efficient coupling of scintillation light, and the Photomultiplier Tube (PMT) is essential (Figure 4). The number of counts in a detector:

$$c = \frac{A\varepsilon\lambda}{4\pi r^2} - b \quad (6)$$

Where;

A: area of detector (m)

λ: source intensity (Bq)

ε: real efficiency of detector

r: distance between source and detector (m)

c: number of counts

b: background count

Then the expected total count in duration T (in seconds),

$$C = T\ \frac{V_S\varepsilon\lambda}{r^2} \quad (7)$$

$$\varepsilon = ev \quad (8)$$

$$V_S = \frac{A}{4\pi} \quad (9)$$

Where;

e: expected efficiency of detector

v: efficiency vector

V_s: constant surface gain

The total count in a detector is inversely proportional to the square of the distance between the detector and the radioactive source, which is known as the Inverse Square Law. This principle is vital to localize the source using a mobile robot because directional information is not available. Hence, the relationship between distance and number of counts is a crucial metric to estimate the location of the source. The size of

detectors directly affects the number of counts captured, and the maximum count is observed if all surfaces of the detector are exposed to radiation. Geometric efficiency defines the ratio between the number of particles propagated by the radioactive source and the number of particles captured by the detector. It is obvious that geometric efficiency increases if all the surfaces of the detector are exposed to radiation. Radiation sources are omnidirectional, so it is hard to extract the one-dimensional information without shielding it in a detector. Activity is another thing affecting the number of counts linearly, which means that more activity yields more counts. Detectors cannot distinguish whether a radioactive source has high activity in a long-distance or has low activity in a short distance. In the presence of multiple radioactive sources, the distinguishability of sources is more complex and harder than estimated.

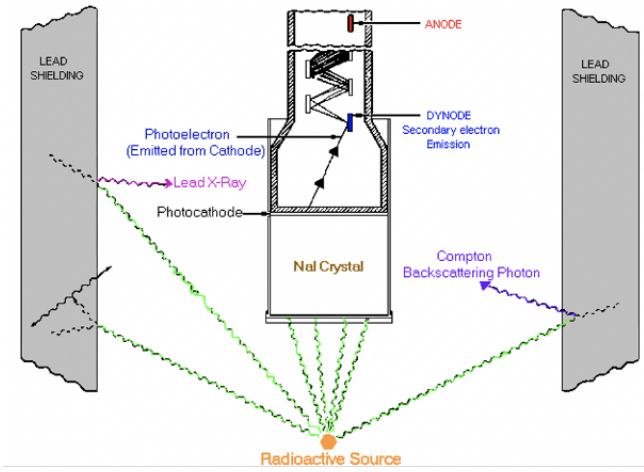

Figure 4. Structure of scintillation detector[37]

2. METHODOLOGY

2.1. Circular Approach

In the literature review, numerous methods to localize the radiation source through autonomous or non-autonomous UAV/UGV have been investigated and summarized. Although robotics and detector technology developments exponentially increase, the accuracy of the localization or even identification still depends on skilled algorithms. Two assumptions were made to develop a new algorithm for better accuracy. The first one is that there is a single source in an unknown and empty environment. The second is assigning the geometric efficiency vector in the detector equation. This vector is any number between zero and one. If one of the maximum count readings is detected, which means that the largest surface of the detector is perpendicularly exposed to radiation, the vector is equal to the one. Since the modeled detector has a cuboid shape, a maximum of three sides are exposed to radiation sources. From the experiments in GazeboSim, the largest side of the detector can read multiple times larger counts than that of the smallest surface. This experiment proves the applicability of the second assumption. The algorithm presented is tested in Gazebo Simulator using a Cs-137 source modeled [31]. The algorithm starts with the first exploration of the environment. A pre-planned zig-zag path is defined for a mobile robot navigated in the map retrieved by manual inspection through the G mapping algorithm. During the first exploration, the robotic platform is responsible for following waypoints assigned by the designer as correct. The Timepix detector counts and records the number of counts captured with the position information in the x-y axis. The first exploration is crucial in the observability of radiation

distribution in initially unknown environments and determining the maximum count readings called hotspots. An example of the first exploration of the environment is illustrated in Figure 5. Once the first exploration is completed, and visual inspection is done, a threshold value or declaration of the number of highest counts to be considered as a reference needs to be specified. The number of reference counts to determine the hotspots is assigned to five as a default.

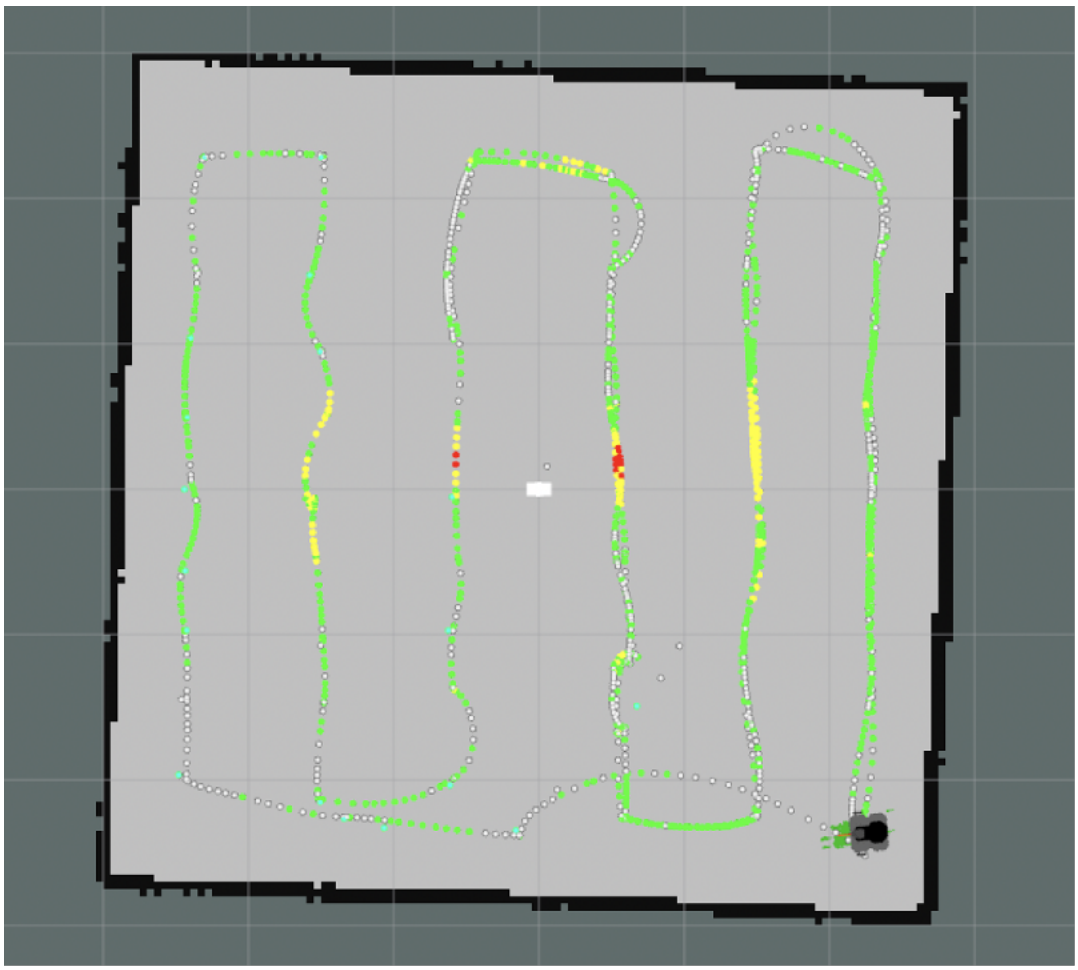

Figure 5. First exploration of environment

Although a predefined path in the map after manual inspection of an unknown environment is notified to the robot, a mobile robot can not perfectly follow the direction desired. Even if the mobile robot is able to follow the path successfully, the orientation of the detector with respect to the source is subject to change so that the desired orientation is not guaranteed. This deficiency is the critical point of the circular approach. We can now consider a maximum count reading during the exploration of the environment once the map is created by manual inspection of the unknown territory. Since the largest surface of the detector is perpendicularly placed to the x-axis of the robotic platform, it is evident that the geometric efficiency vector is equal to one as the largest surface of the detector is orthogonal to the radiation flux. If this information is combined with the obscurity of orientation during measurement, the possible location of the radiation sources draws a circle around the mobile robot. Figure 6 exemplifies why the estimated positions of the source with respect to the detector frame a circle. It is expected that there will be a vast number of count readings during the exploration of the environment, and only the maximum counts need to be determined to filter possible hotspots and draw a circle covering all potential hotspots in x-y space. The average of five counts is calculated, and lower counts within the interval are considered as possible hotspots. On the other hand, it is hard to assign the estimated distance between source and detector without knowing the activity and actual distance. The estimated distance represents the radius of the circles in the circular algorithm. If the path planner were perfectly reliable, it would be clear that the intersection points of circles around hotspots are chosen as a possible

position of the radioactive source. However, consideration of any orientation possibility makes this approach unreliable.

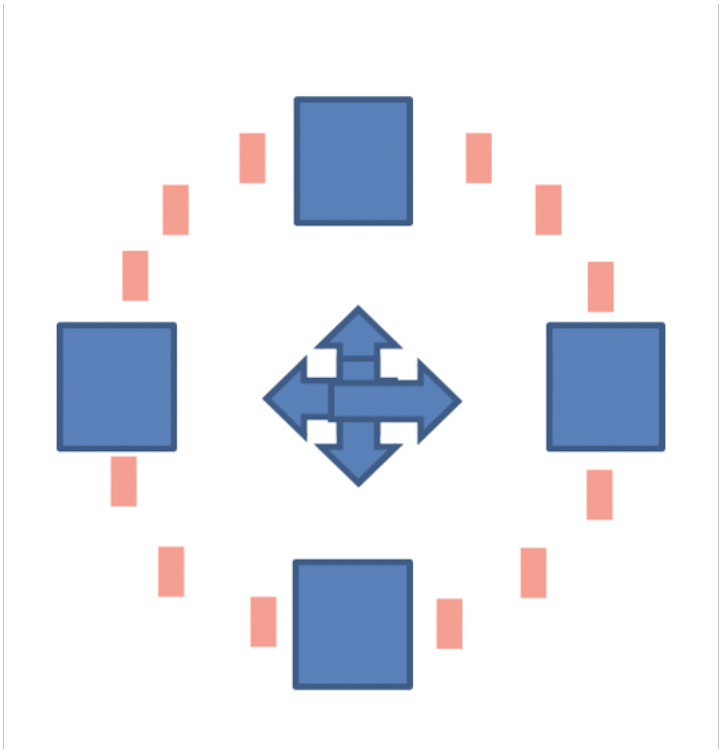

Figure 6. Representation of the circle around mobile robot

The usage of intersections might be fallacious, as explained. However, it provides a higher probability for the areas occupied by the circles of hotspots. The first circular region of interest can be defined by the circle centered by the average position of potential hotspots captured and extracted after the first exploration in the x-y axis with the radius covering all hotspots. One of the most vital properties of the circular approach presented is that the algorithm takes orientational errors into account in order to successfully reduce the region of interest to search for radioactive sources. After the upper limit of radius, a lower limit naturally appears due to the dimensional limitation of the mobile

robot employed. In our case, the dimensional constraint of TurtleBot3 is 0.25 m. Thus, the circular approach offers a solution for the localization problem of a single source with unknown activity. For multi-source scenario, the activity (intensity) of source must be taken into account. If we want to expand the circular approach to the multi-source scenario, we may try to identify the sources respectively. This identification process starts with the calibration of detector using a radioactive isotope with known gamma energy (KeV) such as Cs-137. The identification of gamma sources can be done by the gamma energies (KeV) of different isotopes. Different isotopes can be differently colored using hotspots if the isotopes were identified so that the circular algorithm can be applied. Similarly, if the activity levels are successfully estimated, then the circular algorithm can be employed to cluster the hotspots by measuring the distance between hotspots and comparing the distance between them. However, if the sources are identical, the distance between sources is important.

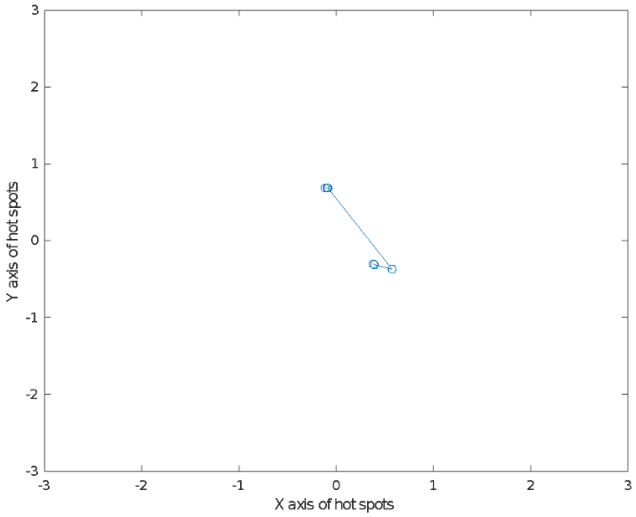

Figure 7. Possible hotspots extracted from all count readings

In case the sources are too close to each other, then the circular approach yields a single circular ROI. This idea is useful for the routine inspection of the environment. The first circular region of interest (ROI) is shown in Figure 8, where the Cs-137 is placed at the origin of the 6x6 square-shape environment. Since the ROI is narrowed to a circle, the required time to localize the source decreases. It is evident that the choice of the mobile platform directly affects the lower limit of the circular approach. For the more giant platforms, it may be considered as a disadvantage of the circular algorithm. The small blue circles in Figure 7 represent the extracted possible hotspots from total counts. These blue circles correspond to peak counts captured during the first exploration shown in Figure 7. Extraction of likely hotspots from all count readings makes the first circular region possible by drawing the circle covering all potential hotspots as defined earlier. In Figure 8, the interpolation of the count readings after the first exploration of environment is illustrated. Figure 10 shows that the perimeter of the circle can intersect the actual position of Cs-137 if the circular region of interest is appropriately compressed and centered iteratively. The compression rate, the radius of the circle, is determined using the inverse square law as new count readings are captured by the mobile robot in the new ROI. The robot is navigated to the inside of the circle to take new counts. The first circular region of interest (ROI) is shown in Figure 10, where the Cs-137 is placed at the origin of the 6x6 square-shape environment. In the lower limit of the circle, the algorithm assumes that all points on the perimeter of the circle are a possible estimation of Cs-137; however, this causes a large interval to test the algorithm's accuracy. In order to annihilate the problem, the probability density function (PDF) of

Normal distribution is employed. After the first exploration, the probability density function is defined and iteratively updated until the dimensional limit is reached. The final PDF provides the highest probability in the smallest ROI as the robot is rotated around itself. The estimation of Cs-137 is reduced to two intersection points due to the reciprocal structure of the detector. A line, which represents the highest probability, intersects the circle in two points. The algorithm regarding the circular methodology is shown in Figure 9.

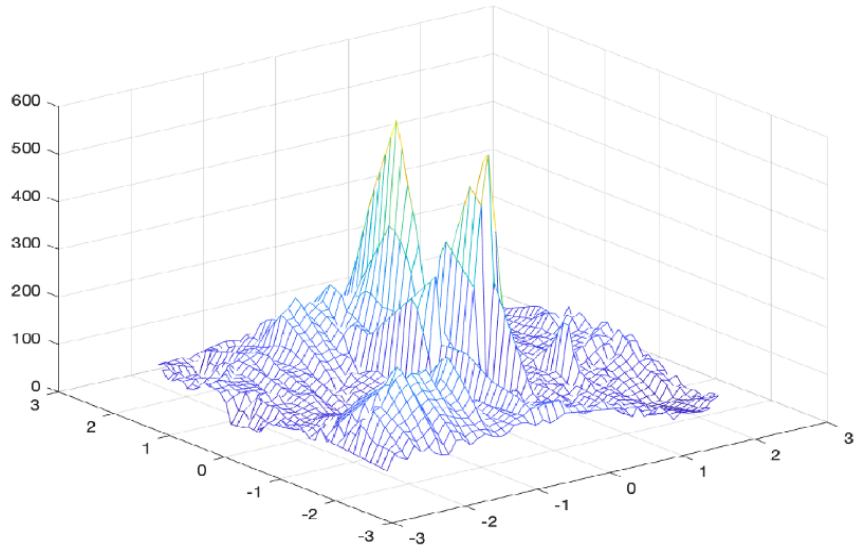

Figure 8. Interpolation of the count readings after the first exploration

The background counts during the experiments are zeroed because very low counts per second are recorded. The background counts generally result from the electronics in the environment. If the background is significantly noisy, higher counts per second are observed. This is not considered as a problem for localization and identification of radioactive sources. However, it would make the quantification of the source

harder. Similarly, if the background count is very high for some reason, it may be detected as a radioactive source, but this is unusual.

1: take first exploration of the environment
2: take three highest readings and calculate σ
3: extract possible h_{p_i} and h_{c_i} inside 1σ, and derive N
4: calculate p_{λ_0}
5: assign $r_{max} = r_0$
6: plot A_{AOI_0} using p_{λ_0} and r_{max}
7: derive P_0 and assign L(P) = P_0
8: **for all** A_{AOI_i} **do**
9: Calculate Δ
10: calculate $p_{\lambda_i}, r_{i+1} = r_i - \Delta$
11: prepare $A_{AOI_{i+1}}$
12: derive P_i
13: compare μ_i and μ_{i-1}
14: **If** $\mu_i > \mu_{i-1} + \sigma$ **do**
15: L(P) = P_i
16: **end if**
17: : **if** $r_i - \Delta \leq r_{min}$ **do**
18: **break**
19: **end if**
20: **end for**
21: Turn around p_{λ_i}, derive highest probability from P_i
22: Assign intersection points as estimated source location
23: return $[s_{ep}\ P_i]$

Figure 9. The circular algorithm

The background count can be also neglected in nuclear facilities. Since there are many uranium sources such as fuel for reactor in such a facility, the detectors record higher counts. The background count in the facility might be relatively higher than that of a normal environment. However, it is still very low when it is compared to the counts from the uranium sources. That's why, the background count can be neglected in almost all situations.

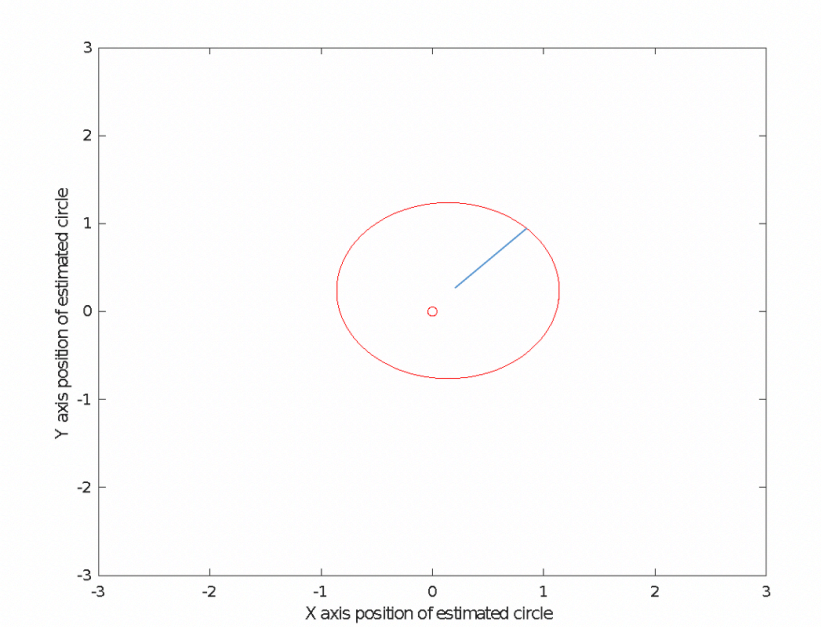

Figure 10. Small red circle in origin represents the position of Cs-137 as the larger circle indicates the smallest circle covering all possible hotspots

2.2. Robotic Platform

The TurtleBot3 Waffle Pi is one of the most popular commercial robots in the market (Figure 11). This mobile robot consists of 2-D LIDAR for SLAM & Navigation and a Raspberry Pi Camera for perception. A Raspberry Pi as Single Computer Board (SCB) is employed to manage the robot. In order to test the circular approach through TurtleBot3 Waffle Pi, some modifications are required. First of all, the Raspberry Pi has been updated to the Nvidia Jetson Nano developer kit due to the utilization of high GPU. Firstly, the Raspberry Pi 4 with 2 GB was employed and then the RAM was gradually increased up to 8 GB. Unfortunately, the Raspberry Pi 4 with 2 GB and 4 GB were not able to run the model in GazeboSim. Then, the version with 8 GB was employed, however, too much lag was observed. The required time to complete the simulation was approximately 234 mins and it was also observed that the system was fully frozen when the

3D LIDAR was activated. Because of the high GPU demand of Gazebo, NVIDIA Jetson was used. Jetson Nano has smaller RAM and an older version of microprocessor. Although it comes with 4 GB RAM and older microprocessor, the algorithm was successfully tested without lag thanks to the GPU in Jetson.

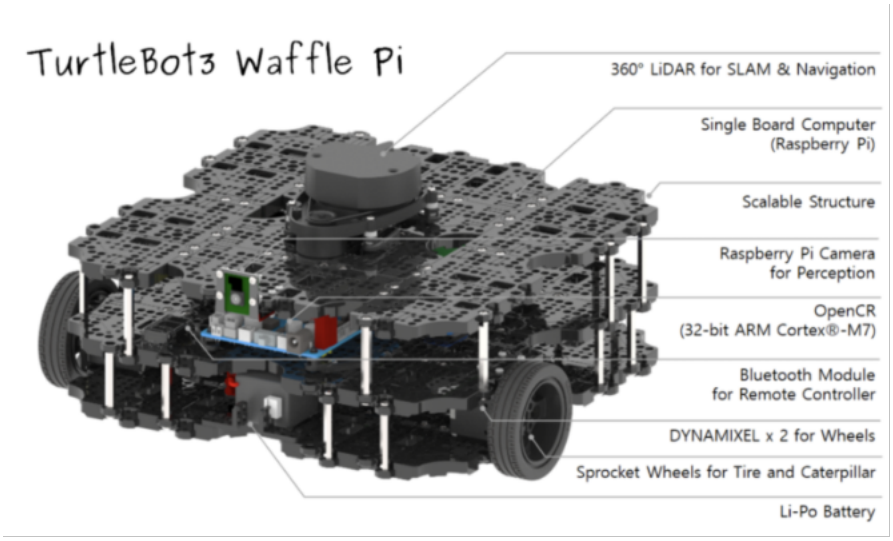

Figure 11. TurtleBot3 Waffle Pi

The algorithm was tested in Jetson Nano and the simulation time was approximately 49 mins. Overall, Jetson NANO with 4 GB does better job than Raspberry with 4 and 8 GB respectively. Hence, the Raspberry Pi 4 in TurtleBot3 needs to be replaced by Jetson NANO for this project. Since the visualization of the environment using 3-D LIDAR is still an expensive technology, a 3-D LIDAR based on rotational 2-D Hokuyo LIDAR through the PhantomX XL-430 robot turret has been designed (Figure 12). The 3-D LIDAR is responsible for the visualization of the environment using the point cloud. Finally, the modeled Timepix detector is mounted in front of the mobile robot. The robot platform used in this research is shown in Figure 13.

Figure 12. HOKUYO LIDAR (left) and PhantomX XL-430 robot turret(right)

The job-sharing of the sensors can be summarized that the default 2-D LIDAR is responsible for mapping and 3-D LIDAR visualizes the environment as the Timepix detector takes the radiation counts. Multiple detectors would be also considered for the verification of the counts. Since radiation is a random event, the verification of the counts by multiple detectors would be beneficial at the expense of higher cost. Multiple detectors would be also placed in different orientations so that the more scan in unit time would be recorded. Since most detectors are heavy and UAVs have low payload capability, usage of multiple detectors in an UAV is rare. More detectors would occupy more place on the platform so it would be problematic for UAVs, as well. The camera is deactivated for this mission.

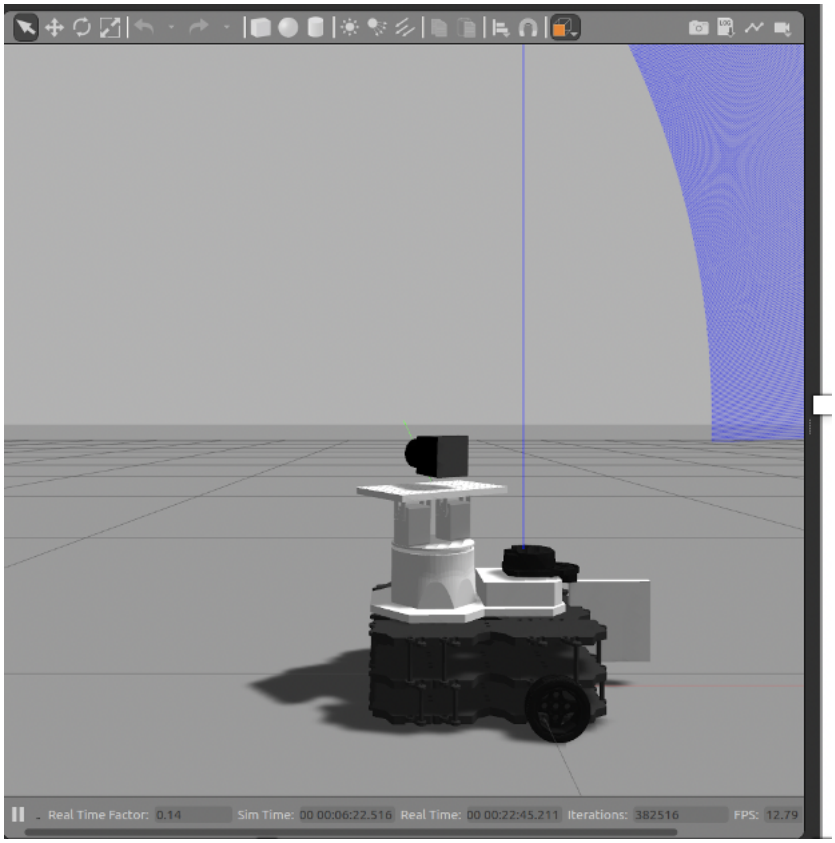

Figure 13. Robotic platform used in the experiments. The TurtleBo3 Waffle Pi modified with rotational LIDAR and Timepix detector

2.3. Experiments

The Gazebo Simulator is used to test the circular algorithm. 6x6 square-shaped environment surrounded by concrete walls is chosen. The environment is obstacle-free and unknown initially, and an Am-241 model is placed to the origin that is subject to change according to the experiment. The top view of the empty environment is illustrated in Figure 14. The manual inspection of the environment is required in order to get the map so that the zig-zag planner through waypoints is assigned. The map of the environment recorded by G mapping is shown in Figure 35. The first exploration of the environment by changing the true position of the radioactive source Am-241 is repeated seven times. The

robot is able to generally follow the waypoints assigned as expected. However, it is recorded that the mobile robot cannot always implement the command derived from the navigation. In such a scenario, manual guidance may be required. As a result of the seven experiments, all the count readings are recorded and plotted in Figure 15 - Figure 21. The possible hotspots are colored red. Once the hotspots with positions are determined, the first circular ROI is drawn. The circular ROI of seven experiments is shown in Figure 22 - Figure 28, respectively. From the visual inspection of Figure 22 - Figure 28, it is clear that the positions of hotspots are close to the true position of the Am-241. Similarly, circular ROI comprises the true position of a radioactive source in most cases, which the visual inspection of Figure 35 can verify. In order to visualize the iterative compression of the first circular ROI, only one scenario is handled. For the iterative experiments, the Am-241 is located to the origin and remains stable during the experiments.

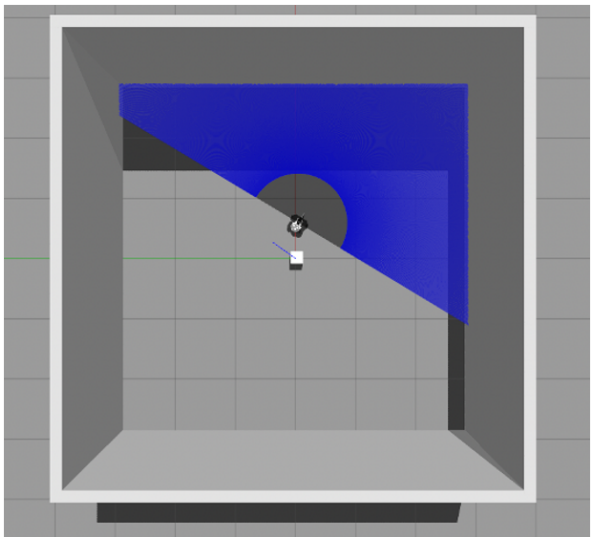

Figure 14. The visualization of environment in Gazebo

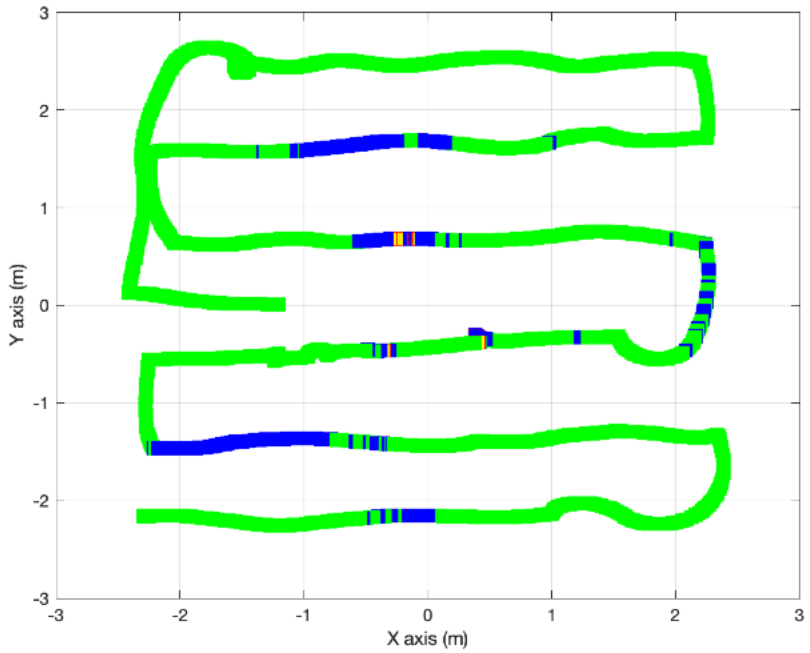

Figure 15. Experiment 1

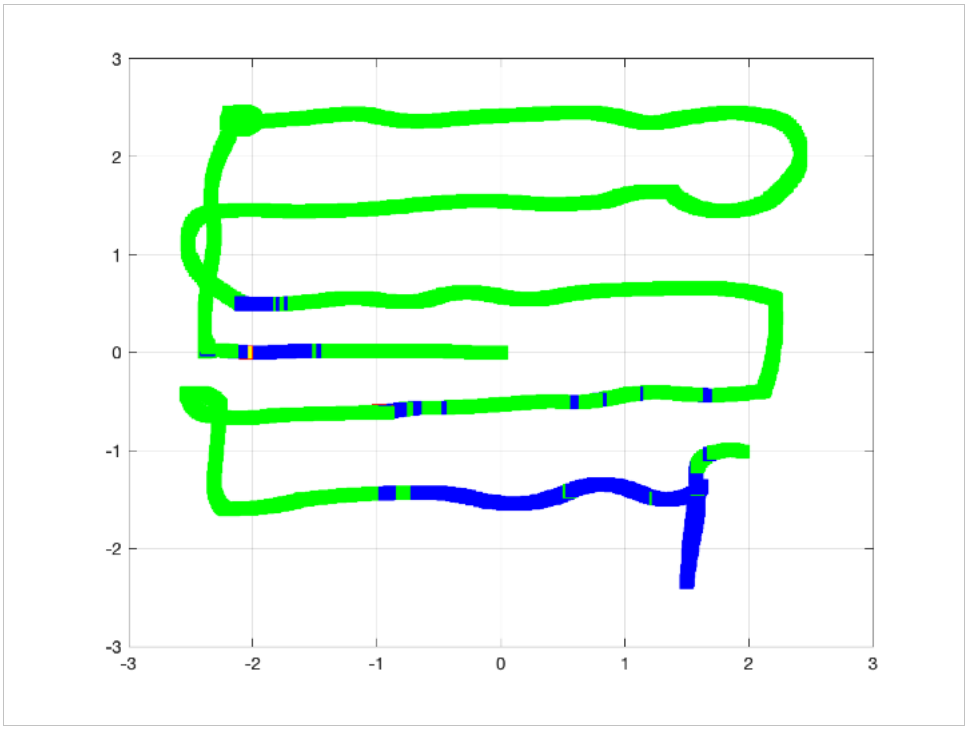

Figure 16. Experiment 2

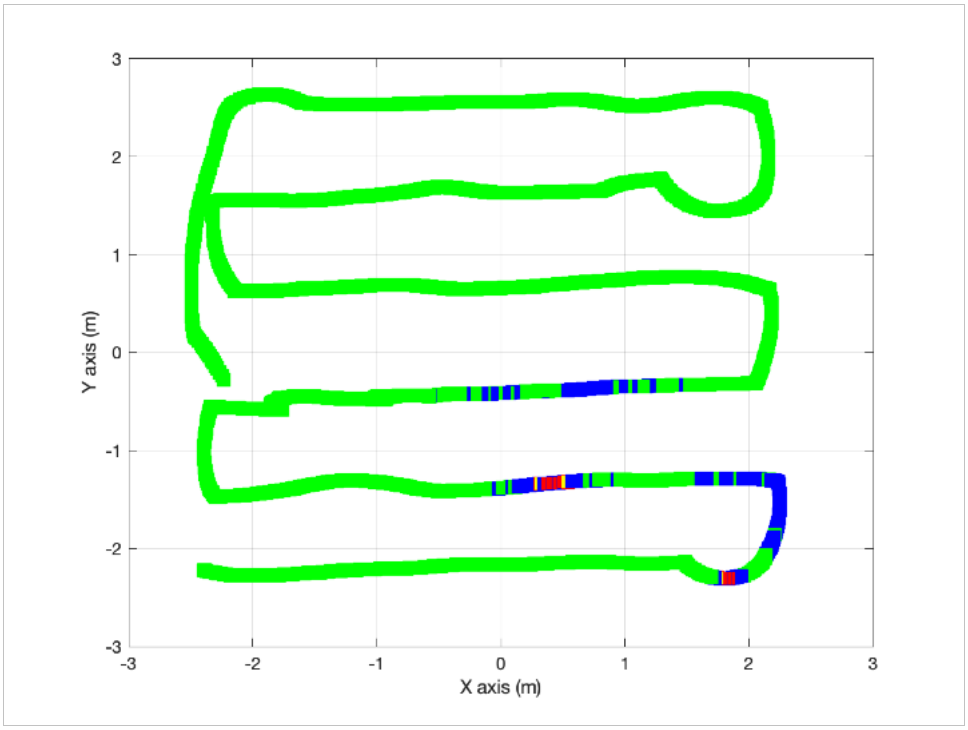

Figure 17. Experiment 3

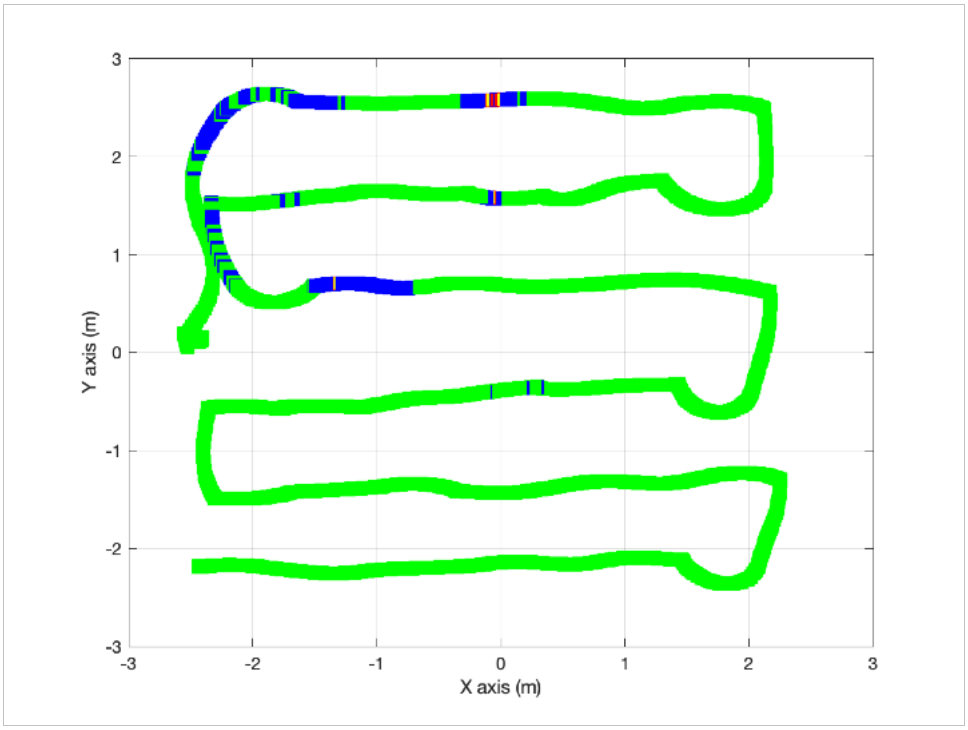

Figure 18. Experiment 4

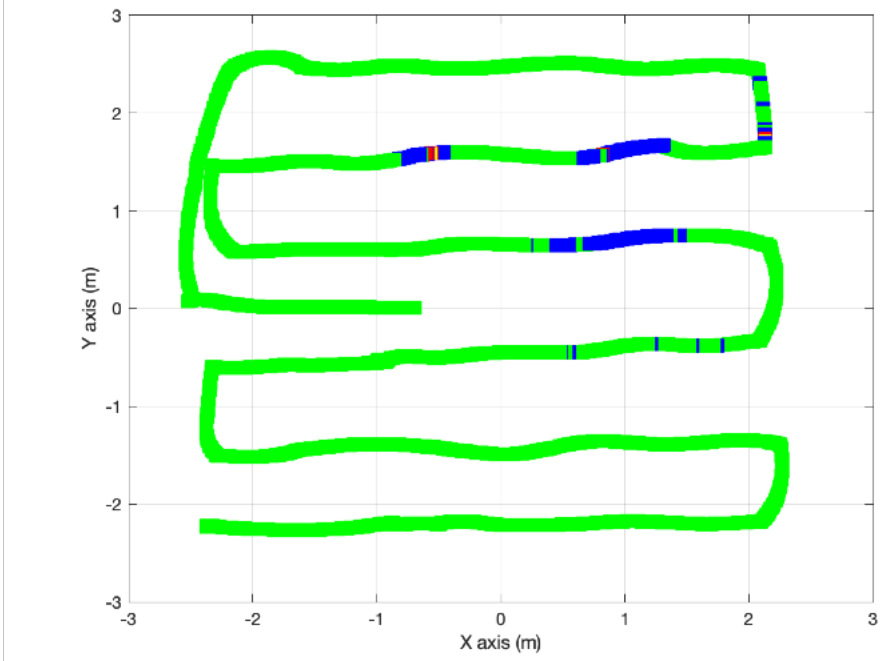

Figure 19. Experiment 5

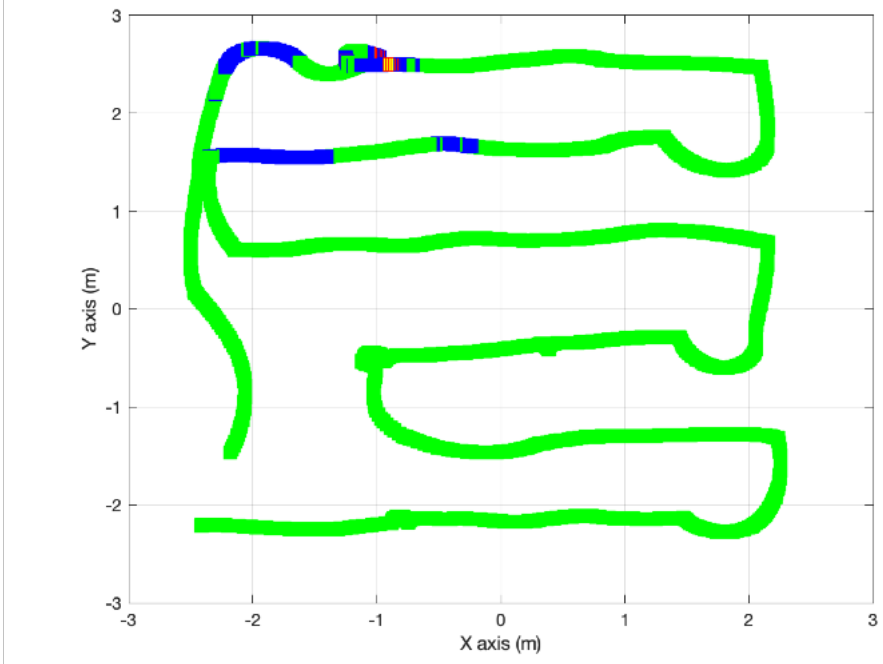

Figure 20. Experiment 6

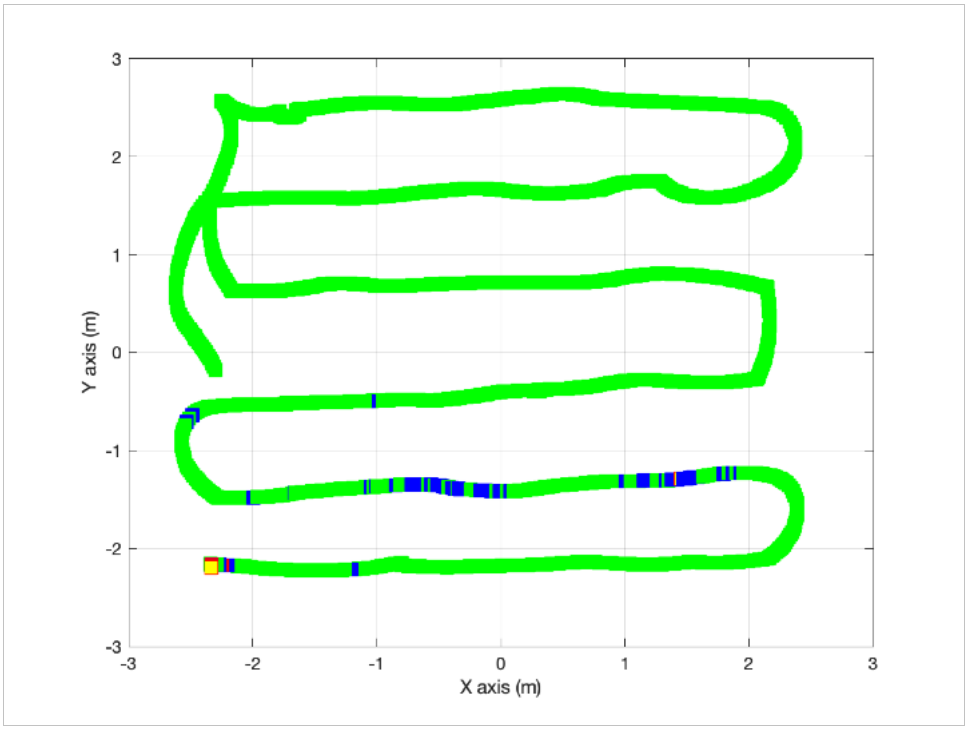

Figure 21. Experiment 7

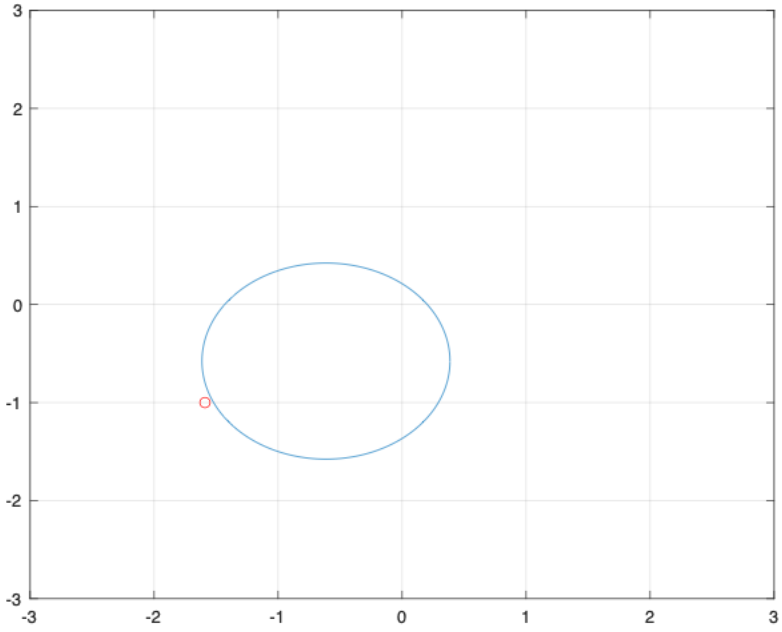

Figure 22. Experiment 1 (Circular ROI)

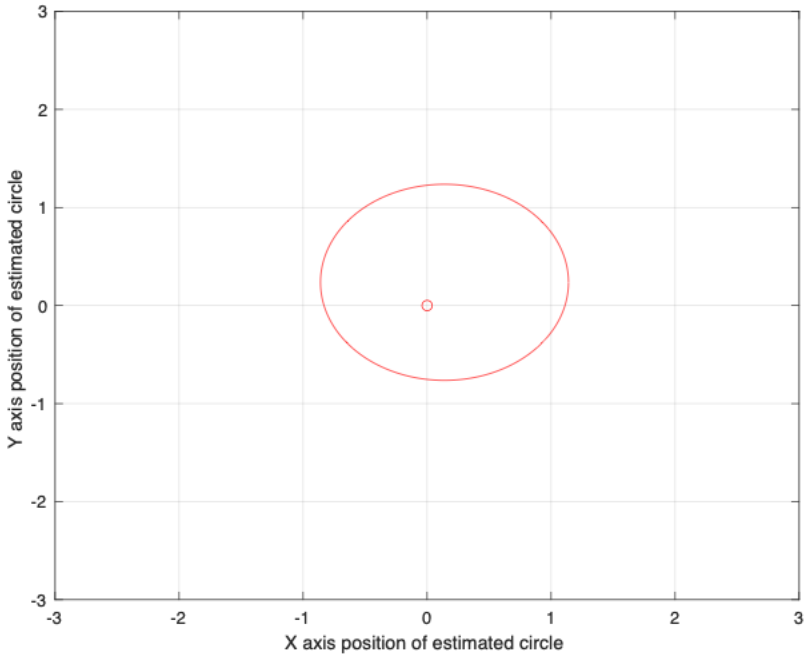

Figure 23. Experiment 2 (Circular ROI)

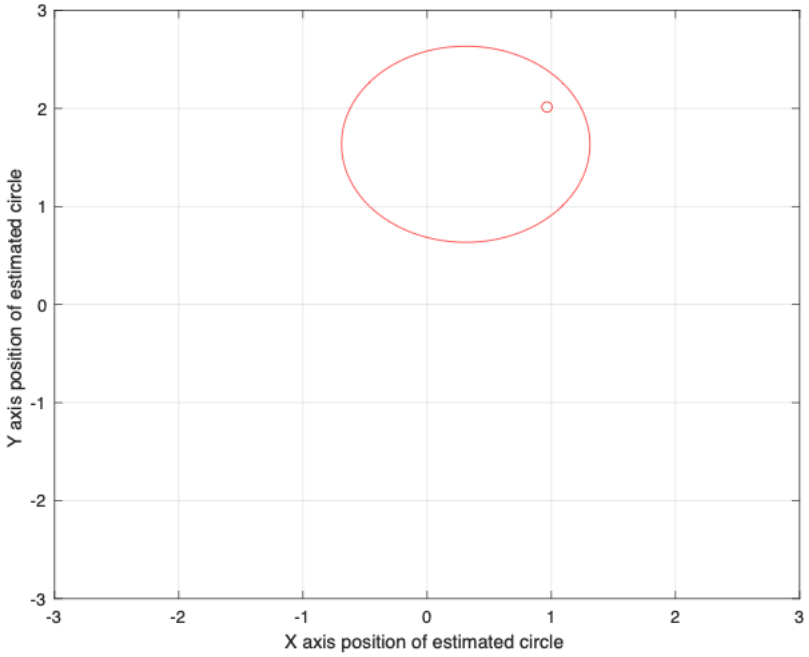

Figure 24. Experiment 3 (Circular ROI)

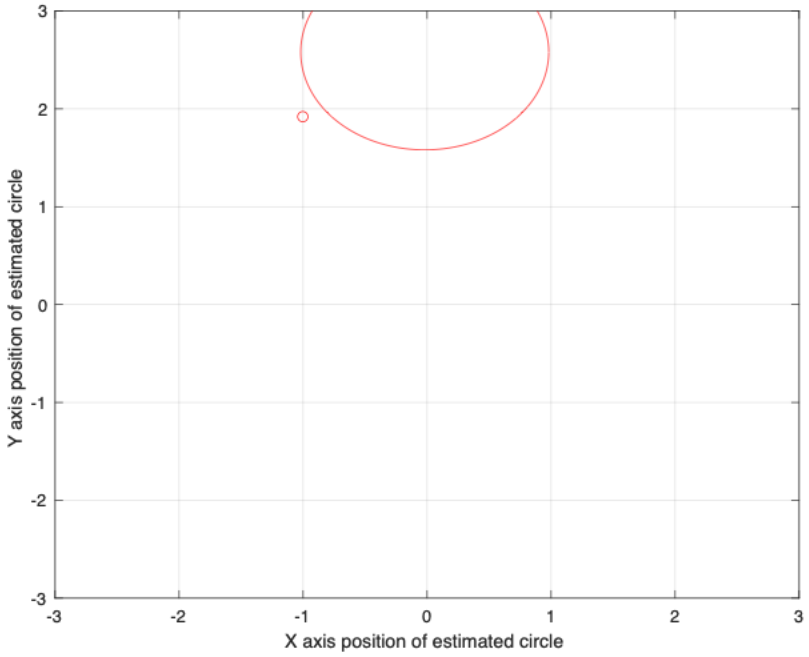

Figure 25. Experiment 4 (Circular ROI)

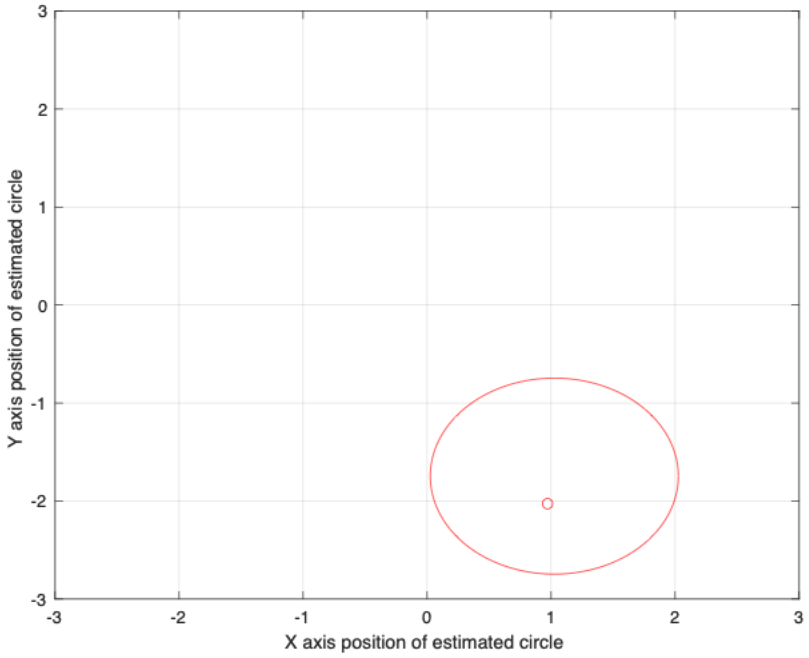

Figure 26. Experiment 5 (Circular ROI)

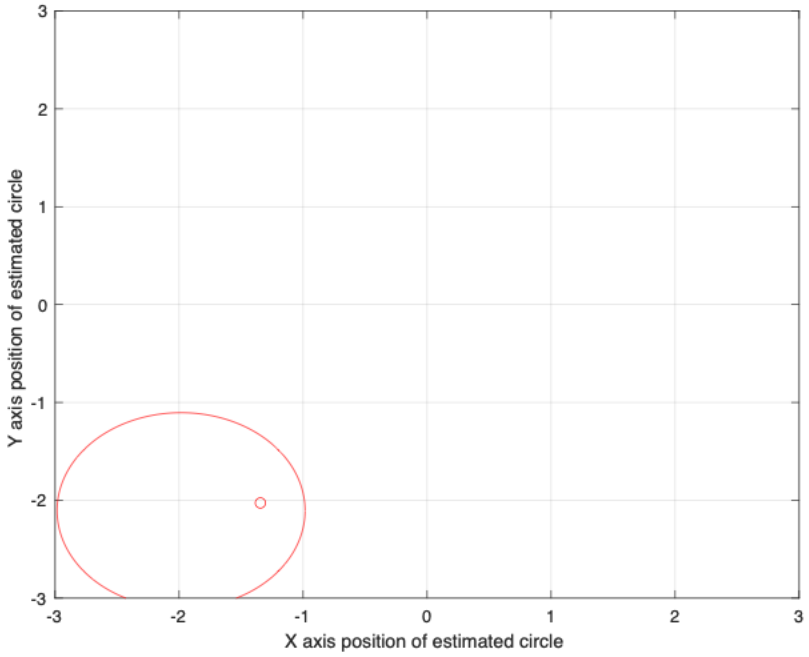

Figure 27. Experiment 6 (Circular ROI)

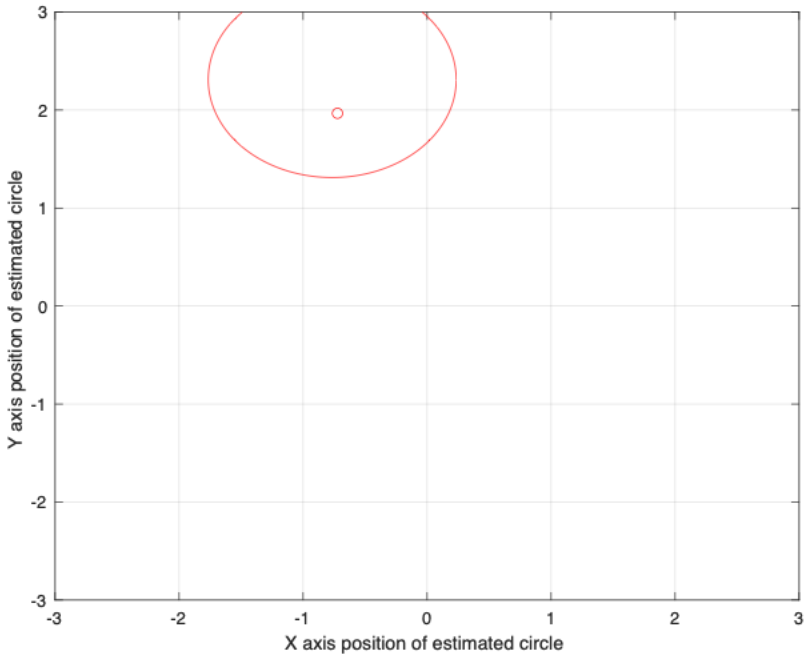

Figure 28. Experiment 7 (Circular ROI)

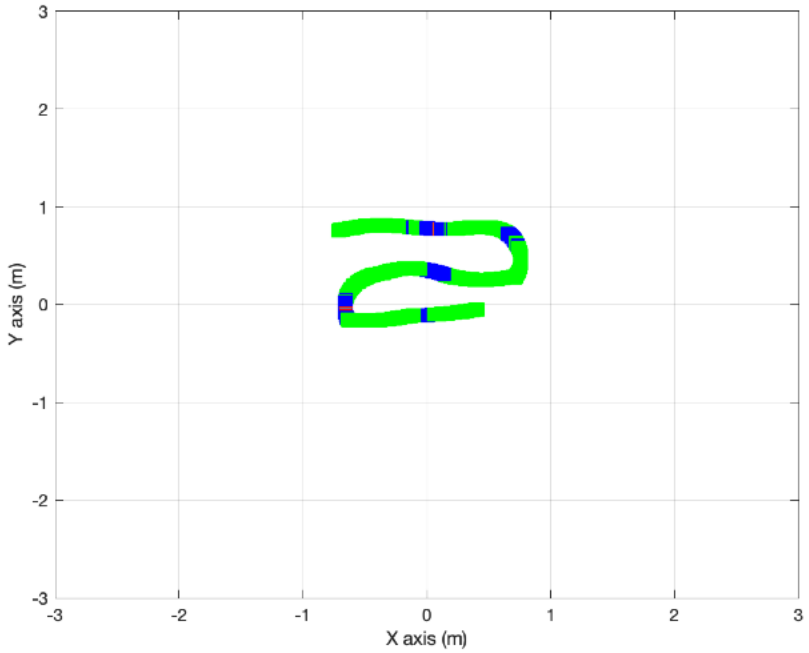

Figure 29. Second iteration of Experiment 1

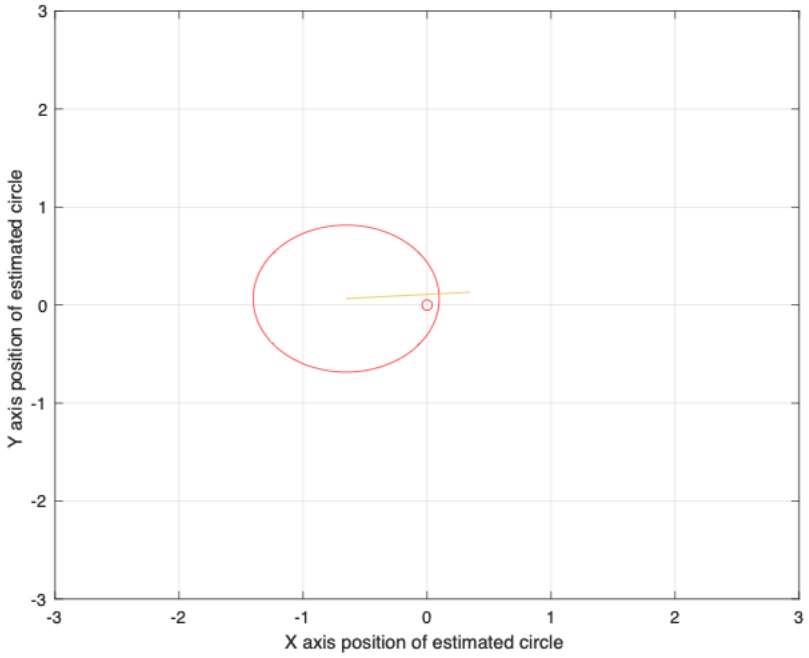

Figure 30. Second iteration of Experiment 1 (Circular ROI)

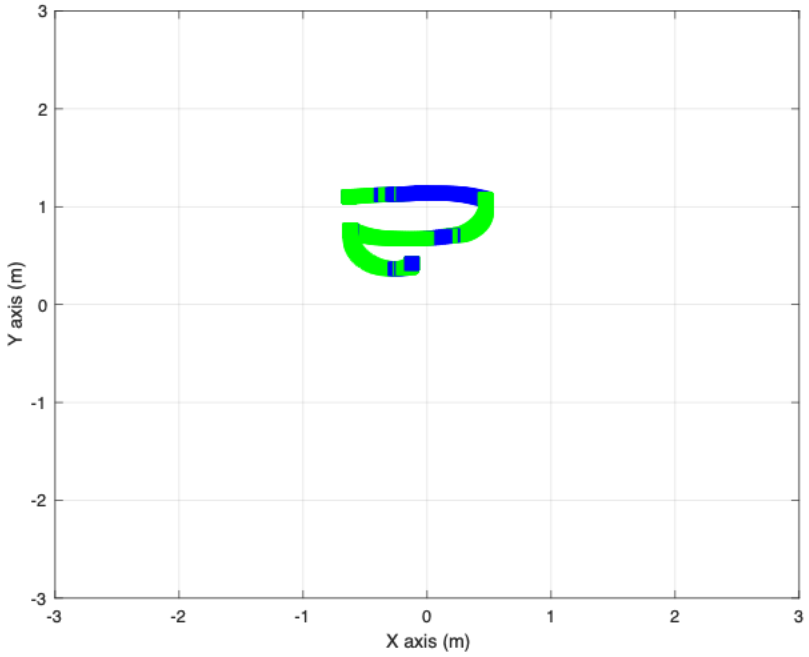

Figure 31. Third iteration of Experiment 1

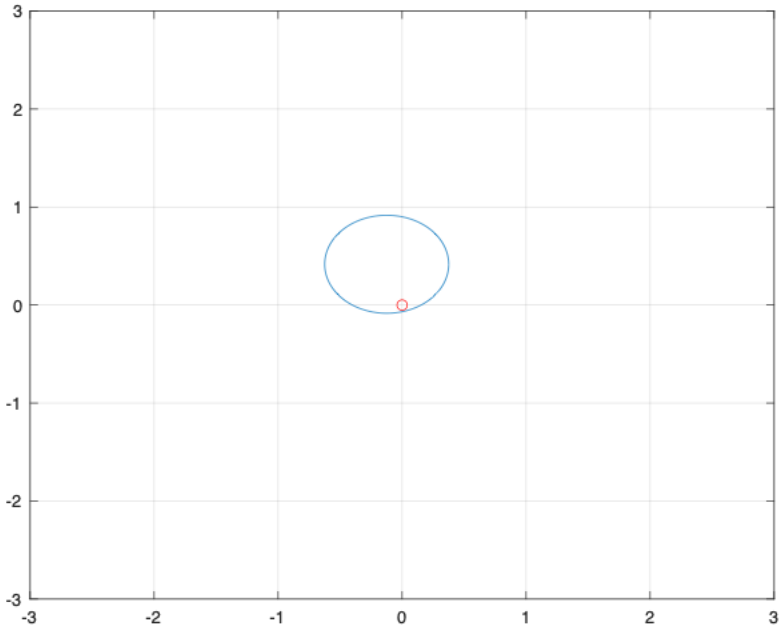

Figure 32. Third iteration of Experiment 1

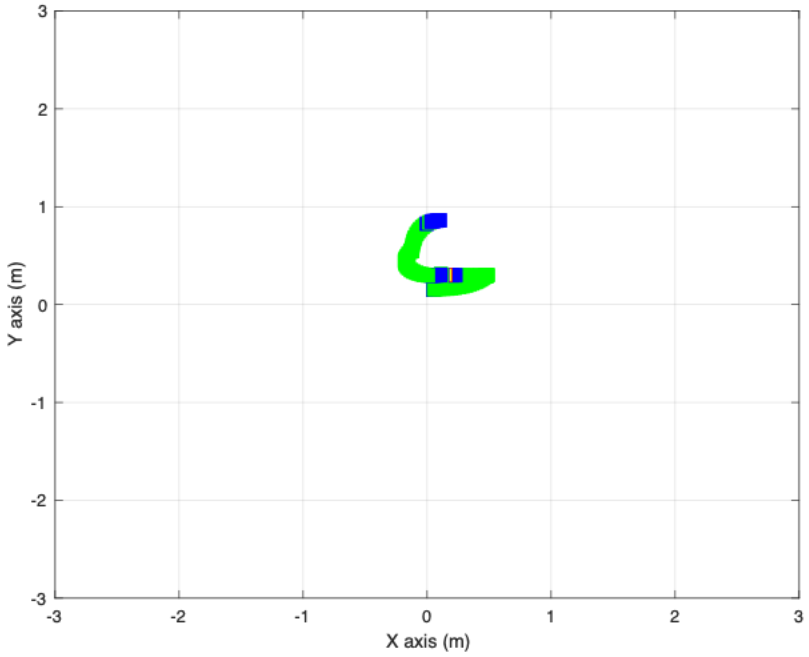

Figure 33. Third iteration of Experiment 1 (Circular ROI)

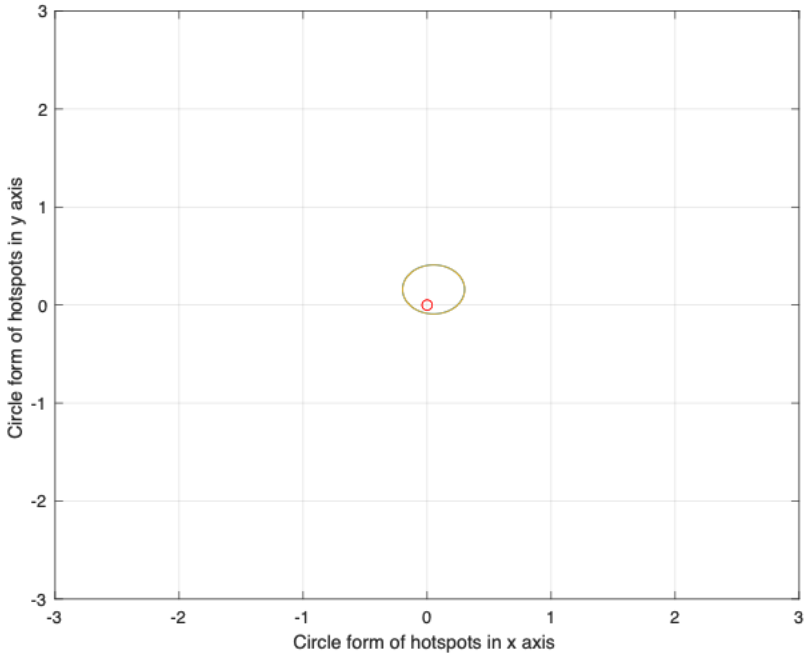

Figure 34. Last iteration of Experiment 1

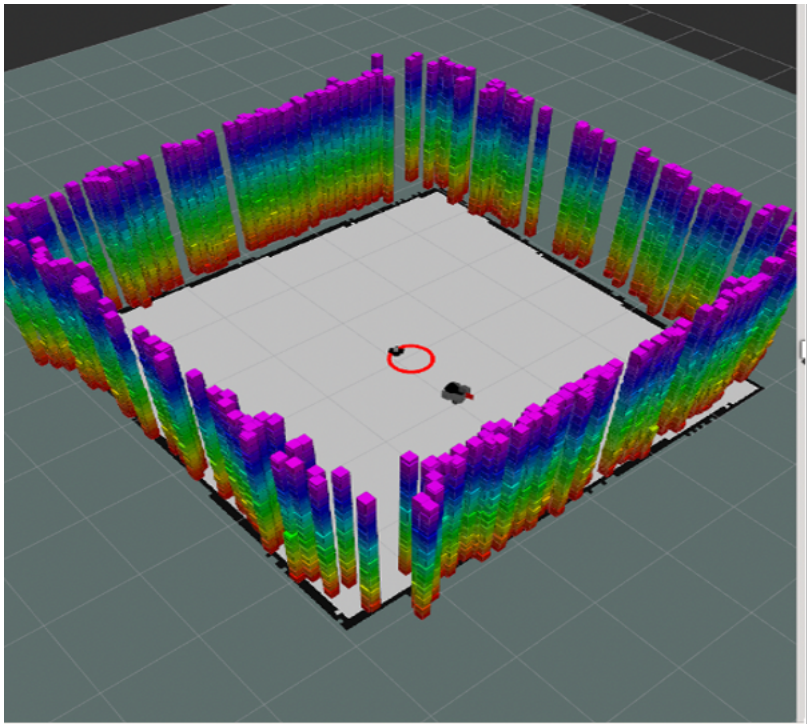

Figure 35. The visualization of the environment

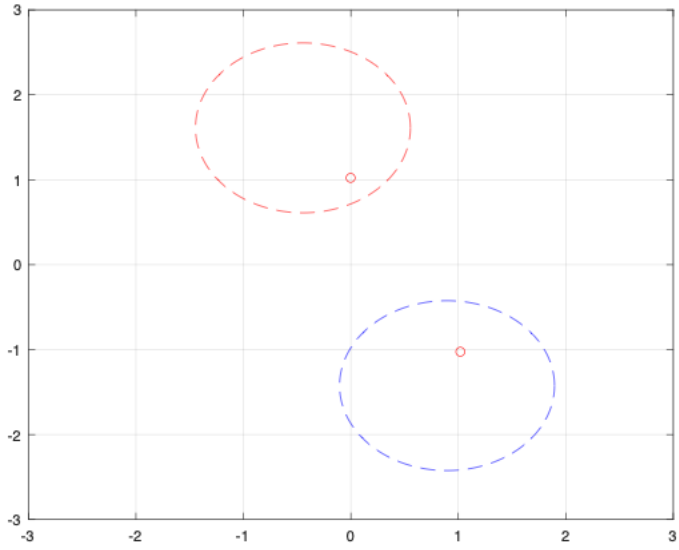

Figure 36. Distance between sources = 2.2361 (meters)

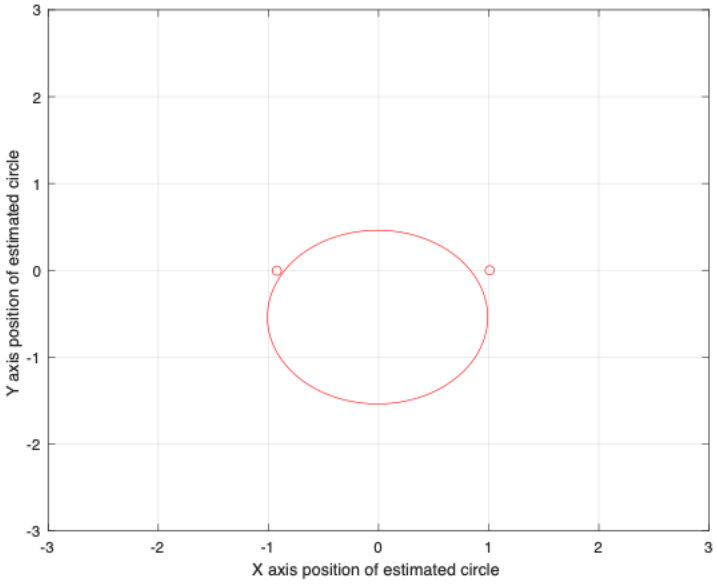

Figure 37. Distance between sources = 2 (meters)

Identical sources (Am-241) are represented by the small red circles. The distance between sources is 2.2361 m and the intensity of sources is 0.5 GBq. The circular algorithm identifies two circular ROI (Figure 36). Similarly, identical sources (Am-241) are represented by the small red circles. The distance between sources is 2 m and the intensity of sources is 0.5 GBq. The circular algorithm can't separate the sources and only one circular ROI is drawn (Figure 37).

3. RESULTS

Five sequential experiments are realized. The accuracy of each experiment is tabulated in Table 1 indicates that the probability of getting an error under 0.25 m is 80%, while there is no error of more than 0.3m. The best result is observed as 0.034 m, as the worst is 0.2629 m. If the best interval is chosen, it can be determined as $0.034 < e < 0.1098$ m. The mean error is 0.165 m. The time to complete the mission is approximately 49 mins, which is assertive among UGVs. Five sequential experiments were performed. The accuracy of each experiment is tabulated in Table 1 where indicates that the probability of getting an error under 0.25 m is 80%, while there is no error of more than 0.3m. The best result is observed as 0.034 m, as the worst is 0.2629 m. If the best interval is chosen, it can be determined as $0.034 < e < 0.1098$ m. The mean error is 0.165 m. The time to complete the mission is approximately 49 mins, which is assertive among UGVs for mapping and localization. The results observed are compared to the results of available studies in the literature. Since there are numerous similar works employing UAV or UGV or both UAV and UGV, a comprehensive comparison is illustrated in Figure 38 and Figure 39. The comparison can be handled in four main branches according to the type of mobile robot employed.

Table 1. Accuracy of five sequential experiments

Experiment	Error (m)
Exp-1	0.2629
Exp-2	0.2003
Exp-3	0.034
Exp-4	0.2202
Exp-5	0.1098

Theoretical methods do not directly apply to a mobile robot, and the accuracy is calculated theoretically. It is evident that UGV has better accuracy than UAV for localization of source as the required time for localization through UAV is significantly less than that of UGV application. Among the UGV applications, the circular method introduced has better accuracy than studies using Recursive Bayesian Estimation and Particle Filter. It offers a very comparable accuracy to that of research having the best accuracy. The applications employing UAV have a significant advantage for the sake of shorter time. Some methods need both UGV and UAV to utilize the pure benefits of mobile robots separately at the expense of increases in computational cost.

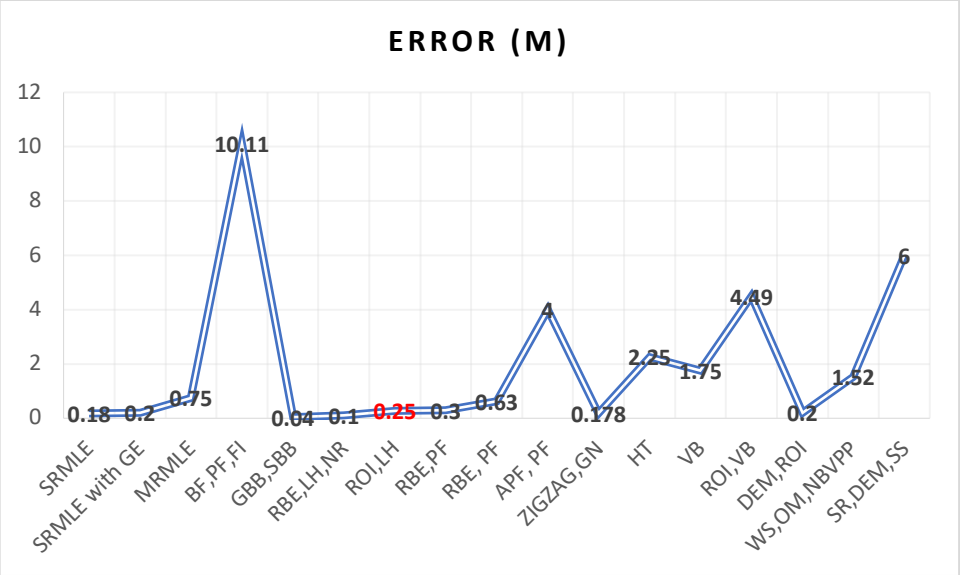

Figure 38. Accuracy comparison: the circular approach versus available approaches

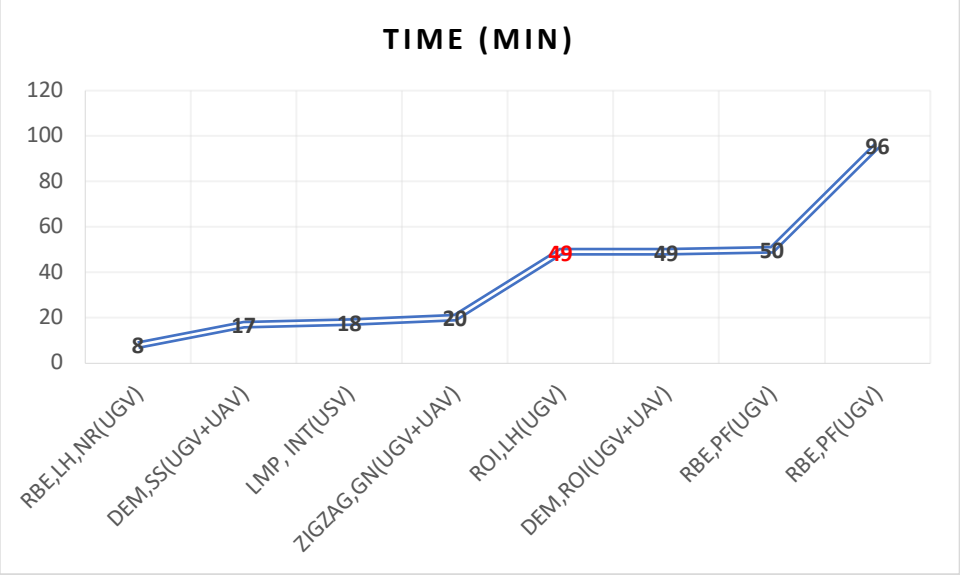

Figure 39. Time comparison: the circular approach versus available approaches

4. SUMMARY AND CONCLUSIONS

4.1. Summary

In this research, an unmanned ground vehicle has been designed to measure the radiation level in an unknown environment to replace human workers with mobile platforms to protect human health from the side effects of radiation. The developed mobile platform is responsible for mapping an unknown environment by manually controlled inspection, visualization of the environment through point cloud through 3-D LIDAR based on rotational 2-D LIDAR, and localizing unknown radioactive sources using a circular approach. A recent study enables researchers to test newly different approaches in Gazebo Simulator, and the model of radioactive sources and the Timepix detector are contributed to the Robot Operating System (ROS) community as open-source, which is one of the main motivations behind this study [31]. The main contribution of this study is to develop an approach called circular approach according to count readings taken and position information of readings. Since the robotic platform can not strictly follow the waypoints assigned by the user, the same orientation in iteration experiments is not guaranteed. Another important point is that a maximum count reading is expected when the largest surface of the detector is exposed to radiation. That is why the reciprocal detector is orthogonally placed in the direction of movement of the mobile robot. The unclarity in the orientation and positioning of the detector in the robot is the starting point of the circular algorithm because the possible source locations around the robot draw a circle around the robot when one of the maximum count readings is captured. It is assumed that the geometric efficiency vector is equal to one if a maximum count is observed.

Hotspots need to be extracted after the first exploration of the environment to be able to draw the circles. However, drawing a circle around each hotspot increases the complexity to reduce the region of interest (ROI) in order to localize the radiation source. Intersection points of circles are handled as the possible position of the radiation source in but this would be reliable if the orientation of the robot was guaranteed [29]. In the case of our design, the orientation is neglected. It is also assumed that the position and activity of the source are unknown initially. The center of hotspots recorded in the (x,y) axis is used as the center of the first circular ROI, and the minimum radius creating a circle covering all hotspots is determined. Thus, the first circular ROI is drawn. The next step of the circular approach is to compress the circle with the right center until the dimensional restriction of the robot is reached. In this study, the simulations of TurtleBot3, Timepix detector, and Phantom pan-tilt in Gazebo are employed to test the approach introduced. Once five experiments are done, the accuracy and time to complete the mission has been recorded and tabulated. The results have been compared to those of similarly available studies in the literature. The cost of the current apparatus in this research is tabulated in Table 2.

Table 2. Cost of the apparatus in the research

Apparat	Cost ($)
TurtleBot3 Waffle Pi	1300
MiniPix EDU with Si Sensor	2500
Hokuyo Scanning Laser Rangefinder	1000
PhantomX XL430 Robot turret	300

4.2. Conclusions

The circular approach presented has been compared to similar studies in the literature regarding accuracy and time requirement. In total, the proposed approach with less than 0.25 m accuracy results in one of the best five methods shown in Figure 35. It also provides a competitive result among the studies using only UGV. Time is an advantage for UAV outdoors at the expense of lower accuracy. The mobile robot with a circular algorithm completes the mission in about 49 mins on average. This duration may be considered as high for 36 m^2. However, usage of UGVs in indoor applications is highly recommended due to restrictions. The trade-off between accuracy and quickness can be balanced according to the requirement of the application. Developments in multi-robot systems with a robust searching algorithm would be the optimal solution of the localization and identification problem of radioactive sources in an unknown environment.

REFERENCES

[1] R. Cortez *et al.*, "Smart radiation sensor management," *IEEE Robot. Autom. Mag.*, vol. 15, no. 3, pp. 85–93, Sep. 2008, doi: 10.1109/MRA.2008.928590.

[2] M. R. Morelande and B. Ristic, "Radiological Source Detection and Localisation Using Bayesian Techniques," *IEEE Trans. Signal Process.*, vol. 57, no. 11, pp. 4220–4231, Nov. 2009, doi: 10.1109/TSP.2009.2026618.

[3] H. E. Baidoo-Williams, "Maximum Likelihood Localization of Radiation Sources with unknown Source Intensity," *ArXiv160800427 Phys.*, Oct. 2016, Accessed: Feb. 27, 2021. [Online]. Available: http://arxiv.org/abs/1608.00427

[4] G. Cordone *et al.*, "Improved multi-resolution method for MLE-based localization of radiation sources," in *2017 20th International Conference on Information Fusion (Fusion)*, Xi'an, China, Jul. 2017, pp. 1–8. doi: 10.23919/ICIF.2017.8009626.

[5] H. Wan, T. Zhang, and Y. Zhu, "Detection and localization of hidden radioactive sources with spatial statistical method," *Ann. Oper. Res.*, vol. 192, no. 1, pp. 87–104, Jan. 2012, doi: 10.1007/s10479-010-0805-z.

[6] J. Han, Y. Xu, L. Di, and Y. Chen, "Low-cost Multi-UAV Technologies for Contour Mapping of Nuclear Radiation Field," *J. Intell. Robot. Syst.*, vol. 70, no. 1–4, pp. 401–410, Apr. 2013, doi: 10.1007/s10846-012-9722-5.

[7] A. Miller, R. Machrafi, and A. Mohany, "Development of a semi-autonomous directional and spectroscopic radiation detection mobile platform," *Radiat. Meas.*, vol. 72, pp. 53–59, Jan. 2015, doi: 10.1016/j.radmeas.2014.11.009.

[8] Abd. H. Zakaria, Y. M. Mustafah, J. Abdullah, N. Khair, and T. Abdullah, "Development of Autonomous Radiation Mapping Robot," *Procedia Comput. Sci.*, vol. 105, pp. 81–86, 2017, doi: 10.1016/j.procs.2017.01.203.

[9] H.-I. Lin and H. J. Tzeng, "Searching a radiological source by a mobile robot," in *2015 International Conference on Fuzzy Theory and Its Applications (iFUZZY)*, Yilan, Taiwan, Nov. 2015, pp. 1–5. doi: 10.1109/iFUZZY.2015.7391884.

[10] F. Hautot, P. Dubart, C.-O. Bacri, B. Chagneau, and R. Abou-Khalil, "Visual Simultaneous Localization And Mapping (VSLAM) methods applied to indoor 3D topographical and radiological mapping in real-time," *EPJ Web Conf.*, vol. 153, p. 01005, 2017, doi: 10.1051/epjconf/201715301005.

[11] K. Vetter *et al.*, "Advances in Nuclear Radiation Sensing: Enabling 3-D Gamma-Ray Vision," *Sensors*, vol. 19, no. 11, p. 2541, Jun. 2019, doi: 10.3390/s19112541.

[12] D. Kim, H. Woo, Y. Ji, Y. Tamura, A. Yamashita, and H. Asama, "3D radiation imaging using mobile robot equipped with radiation detector," in *2017 IEEE/SICE International Symposium on System Integration (SII)*, Taipei, Dec. 2017, pp. 444–449. doi: 10.1109/SII.2017.8279253.

[13] K. Nagatani *et al.*, "Emergency response to the nuclear accident at the Fukushima Daiichi Nuclear Power Plants using mobile rescue robots: Emergency Response to the Fukushima Nuclear Accident using Rescue Robots," *J. Field Robot.*, vol. 30, no. 1, pp. 44–63, Jan. 2013, doi: 10.1002/rob.21439.

[14] I. Tsitsimpelis, C. J. Taylor, B. Lennox, and M. J. Joyce, "A review of ground-based robotic systems for the characterization of nuclear environments," *Prog. Nucl. Energy*, vol. 111, pp. 109–124, Mar. 2019, doi: 10.1016/j.pnucene.2018.10.023.

[15] D. K. Wehe, J. C. Lee, W. R. Martin, R. C. Mann, W. R. Hamel, and J. Tulenko, "10. Intelligent robotics and remote systems for the nuclear industry," *Nucl. Eng. Des.*, vol. 113, no. 2, pp. 259–267, Apr. 1989, doi: 10.1016/0029-5493(89)90077-0.

[16] J. Seyssaud *et al.*, "An humanoid robot for inspections and cleaning tasks in nuclear glove box," p. 7.

[17] D. Kim, H. Woo, Y. Ji, Y. Tamura, A. Yamashita, and H. Asama, "Localization of Radiation Sources Using Gamma-ray Detector in Simulated Environments," p. 2.

[18] A. A. R. Newaz, Sungmoon Jeong, Hosun Lee, H. Ryu, Nak Young Chong, and M. T. Mason, "Fast radiation mapping and multiple source localization using topographic contour map and incremental density estimation," in *2016 IEEE International Conference on Robotics and Automation (ICRA)*, Stockholm, Sweden, May 2016, pp. 1515–1521. doi: 10.1109/ICRA.2016.7487288.

[19] A. A. Redwan Newaz, S. Jeong, H. Lee, H. Ryu, and N. Y. Chong, "UAV-based multiple source localization and contour mapping of radiation fields," *Robot. Auton. Syst.*, vol. 85, pp. 12–25, Nov. 2016, doi: 10.1016/j.robot.2016.08.002.

[20] R. M. Vazquez-Cervantes and F. J. Ramirez-Jimenez, "6-Wheel Terrestrial Robot for Radiation Detection," in *2017 IEEE Nuclear Science Symposium and Medical Imaging Conference (NSS/MIC)*, Atlanta, GA, Oct. 2017, pp. 1–5. doi: 10.1109/NSSMIC.2017.8532653.

[21] T. Lázna, “Autonomous Robotic Gamma Radiation Measurement,” p. 100.

[22] R. B. Andersonl, M. Pryor, and S. Landsberger, “Mobile Robotic Radiation Surveying Using Recursive Bayesian Estimation,” in *2019 IEEE 15th International Conference on Automation Science and Engineering (CASE)*, Vancouver, BC, Canada, Aug. 2019, pp. 1187–1192. doi: 10.1109/COASE.2019.8843064.

[23] R. B. Anderson, M. Pryor, A. Abeyta, and S. Landsberger, “Mobile Robotic Radiation Surveying With Recursive Bayesian Estimation and Attenuation Modeling,” *IEEE Trans. Autom. Sci. Eng.*, pp. 1–15, 2020, doi: 10.1109/TASE.2020.3036808.

[24] B. Ristic, A. Gunatilaka, and M. Rutten, “An information gain driven search for a radioactive point source,” in *2007 10th International Conference on Information Fusion*, Quebec City, QC, Canada, Jul. 2007, pp. 1–8. doi: 10.1109/ICIF.2007.4408041.

[25] J. Huo, M. Liu, K. A. Neusypin, H. Liu, M. Guo, and Y. Xiao, “Autonomous Search of Radioactive Sources through Mobile Robots,” *Sensors*, vol. 20, no. 12, p. 3461, Jun. 2020, doi: 10.3390/s20123461.

[26] C. Ducros *et al.*, “RICA: A Tracked Robot for Sampling and Radiological Characterization in the Nuclear Field: A Tracked Robot for Sampling,” *J. Field Robot.*, vol. 34, no. 3, pp. 583–599, May 2017, doi: 10.1002/rob.21650.

[27] P. Gabrlik and T. Lazna, “Simulation of Gamma Radiation Mapping Using an Unmanned Aerial System,” *IFAC-Pap.*, vol. 51, no. 6, pp. 256–262, 2018, doi: 10.1016/j.ifacol.2018.07.163.

[28] M. Kazemeini, A. Barzilov, W. Yim, and J. Lee, “Gamma Ray and Neutron Sensors for Remote Monitoring Using Aerial Robotic Platforms,” vol. 229, no. 1, p. 8, 2019.

[29] F. Mascarich, T. Wilson, C. Papachristos, and K. Alexis, “Radiation Source Localization in GPS-Denied Environments Using Aerial Robots,” in *2018 IEEE International Conference on Robotics and Automation (ICRA)*, Brisbane, QLD, May 2018, pp. 6537–6544. doi: 10.1109/ICRA.2018.8460760.

[30] F. Mascarich, “Radiation Field Characterization using Autonomous Robots,” p. 51.

[31] P. Stibinger, T. Baca, and M. Saska, “Localization of Ionizing Radiation Sources by Cooperating Micro Aerial Vehicles With Pixel Detectors in Real-Time,” *IEEE Robot. Autom. Lett.*, vol. 5, no. 2, pp. 3634–3641, Apr. 2020, doi: 10.1109/LRA.2020.2978456.

[32] N. Pinkam, S. Jeong, and N. Y. Chong, “Exploration of a group of mobile robots for multiple radiation sources estimation,” in *2016 IEEE International Symposium on Robotics and Intelligent Sensors (IRIS)*, Tokyo, Japan, Dec. 2016, pp. 199–206. doi: 10.1109/IRIS.2016.8066091.

[33] T. Lazna, P. Gabrlik, T. Jilek, and L. Zalud, “Cooperation between an unmanned aerial vehicle and an unmanned ground vehicle in highly accurate localization of gamma radiation hotspots,” *Int. J. Adv. Robot. Syst.*, vol. 15, no. 1, p. 172988141775078, Jan. 2018, doi: 10.1177/1729881417750787.

[34] T. Lazna, “Optimizing the localization of gamma radiation point sources using a UGV,” in *2018 ELEKTRO*, Mikulov, May 2018, pp. 1–6. doi: 10.1109/ELEKTRO.2018.8398368.

[35] M. S. Lee, “Radiation Source Localization using a Gamma-ray Camera,” p. 69.

[36] G. A. Wilde, R. R. Murphy, D. A. Shell, and C. M. Marianno, “A man-packable unmanned surface vehicle for radiation localization and forensics,” in *2015 IEEE International Symposium on Safety, Security, and Rescue Robotics (SSRR)*, West Lafayette, IN, USA, Oct. 2015, pp. 1–6. doi: 10.1109/SSRR.2015.7442944.

[37] G. F. Knoll, *Radiation detection and measurement*, 4th ed. Hoboken, N.J: John Wiley, 2010.